Sustainable Polymer & Energy

SCIEPublish

Review

Structural Design and Application of Two-Dimensional Electromagnetic Wave Absorption and Shielding Materials

Chao Liu [1], Qi Liu [1], Lushen Xu [1], Zheng Fan [1], Qin Meng [2] and Guoliang Zhang [1,*]

[1] Center for Membrane and Water Science & Technology, Institute of Oceanic and Environmental Chemical Engineering, Collaborative Innovation Center of Membrane Separation and Water Treatment of Zhejiang Province, Zhejiang University of Technology, Hangzhou 310014, China; 2112001198@zjut.edu.cn (C.L.); 221124250152@zjut.edu.cn (Q.L.); xulusen@zjut.edu.cn (L.X.); fanzh@zjut.edu.cn (Z.F.)

[2] College of Chemical and Biological Engineering, State Key Laboratory of Chemical Engineering, Zhejiang University, Hangzhou 310027, China; mengq@zju.edu.cn (Q.M.)

* Corresponding author. E-mail: guoliangz@zjut.edu.cn (G.Z.)

Received: 16 March 2026; Revised: 27 March 2026; Accepted: 23 April 2026; Available online: 9 May 2026

ABSTRACT: Electromagnetic waves are the foundation of modern communication and information transmission which take advantage of strong penetration and fast propagation. To prevent electromagnetic radiation pollution and improve application efficiency, the development of new types of electromagnetic wave absorption and shielding materials that can convert electromagnetic wave energy into thermal energy for absorption and shielding has become increasingly important. Although progress in different electromagnetic wave-absorbing and shielding materials is exciting, there are few reviews of new materials, especially two-dimensional materials. By analyzing the structure and loss mechanism of two-dimensional materials, this review systematically summarizes the current research status and unique advantages of two-dimensional materials in electromagnetic wave absorption and shielding. By extending traditional synthetic two-dimensional materials to natural two-dimensional mineral materials, the potential applications of these materials in future green development havee been explored. Based on different application scenarios, new challenges and future directions for highly efficient electromagnetic wave absorption and shielding materials are presented. The prospects for the development of two-dimensional materials are also clarified from aspects of macroscopic and microscopic structural design and functional integration.

Keywords: Electromagnetic waves; Absorption; Shielding; Two-dimensional materials; Structural design

1. Introduction

Electromagnetic waves (EMW) possess the advantage of efficient communication, which has greatly promoted the progress of human society and provided a solid foundation for advanced technological fields such as national defense, aviation, and medicine [1–4]. However, the potential harm to the human body and the interference effects on electronic devices that EMW may cause have made people increasingly attach importance to necessary protective measures and functional materials [5–8]. Among them, the process of

absorbing and shielding EMW through specific materials is regarded as the most effective countermeasure against the hazards of EMW at present [9–11].

The development of EMW absorption and shielding materials is closely related to the evolution of electronic technology and military demands. The early EMW shielding materials were mainly made of metallic materials, which achieved shielding of EMW through reflection. With the increasing demand for radar detection, specific materials such as ferrites and carbon powders that can absorb EMW and convert them into heat energy have become the focus of research [12–14]. With the advancement of technology for multifunctional EMW protection, the integration of multifunctional EMW absorption and shielding materials has become a big necessity [15–18]. In order to meet the high EMW protection standards required, people have focused on exploring new structures or new synthetic methods for materials at present.

Two-dimensional (2D) materials are one of the widely used materials in EMW absorption and shielding materials, which possess many advantages such as large specific surface area, excellent dielectric properties, and vacancy defects [19–22]. Their specific characters make the 2D materials inherently possess good EMW absorption properties. When 2D materials with unique multi-layer structures are combined with other metals or magnetic materials, they can achieve very attractive EMW absorption and shielding effects. All these make 2D EMW absorption and shielding materials a research hotspot in the fields of civilian and military uses [23–25]. So far, although there have been many advancements in the research on 2D materials in EMW AS, there are few comprehensive reviews that include both 2D synthetic materials and mineral materials, especially 2D natural mineral materials. In this regard, we think it is urgent to conduct a systematic review on the structural design, loss mechanism, and specific applications of 2D EMW absorption and shielding materials, which may provide useful theoretical support and design basis for the green development of EMW protection materials.

This review first provides a comprehensive explanation of the loss mechanisms of 2D materials in EMW absorption and shielding, establishing the theoretical basis for the design of these materials. Second, by analyzing the characteristics and advantages of different 2D materials, the key points of structural design in principle are clarified. Third, to open up new routes for the effective utilization of economical fillers in functional composite materials with sustainability, the functionalization design and the synthesis with 2D natural minerals in EMW absorption and shielding are discussed in detail. Recent progresses on the application of 2D EMW absorption and shielding materials is comprehensively summarized. Finally, new challenges and future directions on the development of highly efficient 2D EMW absorption and shielding materials are presented.

2. Mechanism of Electromagnetic Wave Loss in 2D EMW Absorption and Shielding Materials

When EMW enters the surface of a material, three phenomena usually occur: reflection, absorption, and transmission. The key to achieving EMW absorption and shielding lies in absorbing and reflecting the EMW to the greatest extent, converting them into thermal energy, minimizing the transmission of the EMW, and thus protecting the internal objects [26].

The shielding effectiveness (SE) is usually used to measure the shielding performance of materials against EMW, which is defined as the logarithmic function of the ratio of incident power density to transmitted power density [27]. The formula is as follows:

$$SE = 10\,log\left|\frac{P_i}{P_t}\right| = 20\,log\left|\frac{E_i}{E_t}\right| = 20\,log\left|\frac{H_i}{H_t}\right| \quad (1)$$

where P_i and P_t are the incident and transmitted power densities; E_i and E_t denote the incident and transmitted electric field intensities; H_i and H_t stand for the incident and transmitted magnetic field intensities, respectively.

In addition to the aforementioned absorption loss and reflection loss, there are also multiple reflection losses in the electromagnetic wave shielding mechanism. Hence, the *SE* can be expressed as the sum of the reflection loss (SE_R), absorption loss (SE_A), and multiple reflection loss (SE_M) (Figure 1). The expressions are as follows [28,29]:

$$SE = SE_R + SE_A + SE_M \tag{2}$$

$$SE_R = 39.5 + 10\,log\left|\frac{\sigma}{2\pi f\mu}\right| \tag{3}$$

$$SE_A = 8.7d\sqrt{\pi f\mu\sigma} \tag{4}$$

$$SE_M = 20\,log\left(1 - e^{-\frac{2d}{\delta}}\right) \tag{5}$$

where σ represents the electrical conductivity, μ represents the magnetic permeability. f, d, and δ respectively denote the frequency of the EMW, the thickness of the shielding material, and the skin (or penetration) depth.

From Equation (3), the reflection loss of EMW is directly proportional to the conductivity of the material and inversely proportional to its magnetism. Therefore, materials with weak magnetism and high conductivity are crucial for enhancing reflection loss. For some non-magnetic metals, such as gold, silver, and copper, they are the best materials for achieving high reflection loss. However, merely reflexive actions can also cause secondary pollution of EMW, which does not meet the actual application requirements and environmental protection standards. Therefore, the absorption function of EMW is an indispensable aspect in material design. For absorption loss, the primary mechanisms are magnetic loss and dielectric loss, which arise from interactions between the electromagnetic field and the electric or magnetic dipoles within the material. As indicated by Equation (4), with a fixed material thickness and EMW frequency, the absorption loss is proportional to both the electrical conductivity and the magnetism of the material. Consequently, incorporating a higher content of conductive and magnetic components can effectively enhance absorption performance. Multiple reflection loss generally refers to the loss that occurs when EMW is reflected and absorbed multiple times at material interfaces, then converted into heat energy. This loss mechanism usually requires a specific layered material structure to form a large number of adjacent layered interfaces. This is also a unique advantage that 2D materials possess in the field of EMW absorption.

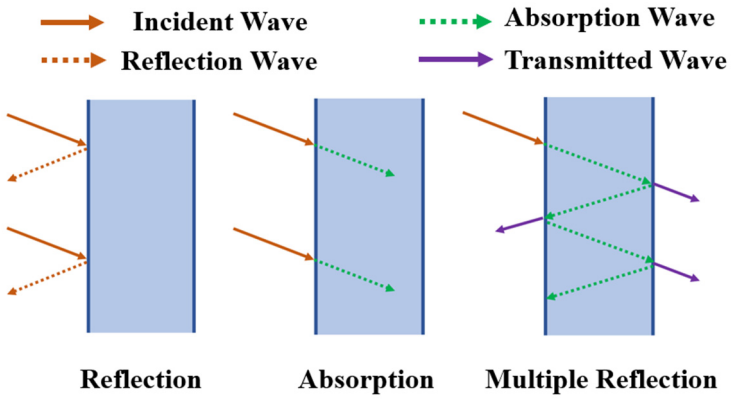

Figure 1. The mechanism of EMW absorption and shielding in the material.

In practical applications, the ability to effectively absorb EMW while minimizing reflection and transmission is crucial. Evaluating absorbing materials solely based on their SE does not accurately represent their real-world performance. The performance of absorption of EMW primarily depends on

impedance matching, which reduces reflection and enables strong electromagnetic attenuation through absorption. According to Maxwell's equations, the response of the absorber to EMW is closely related to the complex permittivity (ε_r) and the complex permeability (μ_r) [30]. The specific equations are as follows:

$$\varepsilon_r = \varepsilon' - \varepsilon'' \tag{6}$$

$$\mu_r = \mu' - \mu'' \tag{7}$$

where ε' and μ' represent the real parts of the permittivity and permeability, respectively, reflecting the material's ability to store electromagnetic energy. The loss factors ε'' and μ'' represent the corresponding imaginary parts, which characterize the material's dissipation of EMW energy. To achieve optimal absorption performance and minimize surface reflection loss, the material's input impedance must be matched to the free-space impedance, thereby maximizing the transmission of EMW into the material. When a transverse wave propagates in a homogeneous medium, the wave impedance is equal to the intrinsic impedance of the medium, which is denoted by the symbol Z_i. The calculation formula is as follows:

$$Z_i = \sqrt{\frac{\mu}{\varepsilon}} = \sqrt{\frac{\mu_0 \mu_r}{\varepsilon_0 \varepsilon_r}} \tag{8}$$

where μ, μ_0, μ_r represent the magnetic permeability of the material, the vacuum magnetic permeability, and the relative magnetic permeability, respectively. ε, ε_0, ε_r denote the permittivity of the material, the vacuum permittivity, and the relative permittivity, respectively. In order to accurately measure the absorption performance of EMW, the academic community introduced reflection loss (RL). The RL value is determined based on the relative complex permeability and relative complex permittivity at a specific frequency and material thickness. The specific formula is as follows [31,32]:

$$RL = 10\, log \frac{P_R}{P_I} = 20\, log \left| \frac{Z_{in} - Z_0}{Z_{in} + Z_0} \right| \tag{9}$$

where P_I represents the incident power of the EMW, while P_R represents the reflected power of the EMW. Z_{in} and Z_0 respectively denote the absorption impedance and the free-space impedance. Usually, the RL value for measuring the absorption of EMW is negative. Therefore, the more negative the RL value is, the higher the reflection degree is. According to the single-layer absorber transmission line theory, Z_{in} can be defined as [33,34]:

$$Z_{in} = Z_i\, tanh(\gamma d) = Z_0 \sqrt{\frac{\mu_r}{\varepsilon_r}} tanh(\gamma d) \tag{10}$$

$$\gamma = j \cdot 2\pi f \sqrt{\varepsilon \mu} = j \cdot 2\pi f \frac{\sqrt{\varepsilon_r \mu_r}}{c} \tag{11}$$

where γ represents the propagation constant of the EMW, j is the imaginary unit, and c is the propagation speed of the EMW. In an ideal absorption-dominant electromagnetic interference (EMI) shield, the ratio of input impedance to free-space impedance, $|Z_{in}/Z_0|$, should approach 1. This indicates that nearly all incident EMW enters the material and is dissipated without significant reflection. While achieving perfect impedance matching is challenging, a key design strategy for such EMI shielding structures is to use materials with closely matched values of μ_r and ε_r.

When evaluating the performance of the absorption of EMW, the attenuation capability of the absorber for penetrating EMW also needs to be taken into consideration. The stronger the material's ability to dissipate energy, the easier it is to convert EMW into heat and dissipate it. Therefore, RL is always explained together with α, where α quantifies the attenuation capability of the structure [35,36]:

$$\alpha = \frac{\sqrt{2}\pi f}{c} \times \sqrt{(\mu''\varepsilon'' - \mu'\varepsilon') + \sqrt{(\mu''\varepsilon'' - \mu'\varepsilon')^2 + (\mu'\varepsilon'' + \mu''\varepsilon')^2}} \tag{12}$$

$$\varepsilon'' \approx \frac{\sigma}{2\pi f \varepsilon_0} \tag{13}$$

where ε_0 represents the vacuum permittivity. The above Equation (12) indicates that the attenuation constant of EMW is directly related to the complex permittivity and complex permeability. For dielectric loss, it dissipates the EMW energy through the movement of electric dipoles and charge carriers. Dielectric loss mainly consists of two main aspects: the conductive loss caused by the movement of electrons, such as jumping and migration, and the polarization relaxation loss, mainly including dipole polarization and interface polarization. From Equation (13) of the free-electron theory, the electrical conductivity of the material increases the conductive loss of EMW, thereby increasing the dielectric loss. For polarization relaxation loss, the Cole-Cole semicircle and Debye relaxation theory can be used to analyze these polarizations and the related relaxation phenomena [37–40]:

$$\varepsilon' = \varepsilon_\infty + \frac{\varepsilon_s - \varepsilon_\infty}{1 + (2\pi f)^2 \tau^2} \tag{14}$$

$$\varepsilon'' = \varepsilon_p'' + \varepsilon_c'' = \frac{2\pi f \tau (\varepsilon_s - \varepsilon_\infty)}{1 + (2\pi f)^2 \tau^2} + \frac{\sigma}{2\pi f \varepsilon_0} \tag{15}$$

$$\left(\varepsilon' - \frac{(\varepsilon_s + \varepsilon_\infty)}{2}\right)^2 + (\varepsilon'')^2 = \left(\frac{\varepsilon_s - \varepsilon_\infty}{2}\right)^2 \tag{16}$$

where ε_s and ε_∞ respectively represent the permittivity in static conditions and at infinite frequency. Additionally, τ is the relaxation time (in seconds). In this context, the relaxation time refers to the specific duration for a polarizing substance to transition from the polarized state to the normal state. ε_p'' and ε_c'' represent the energy dissipation of the material for EMW in the form of polarization and conduction, respectively. For 2D composite materials, dipole polarization is mainly caused by factors such as lattice defects and heteroatoms doping; interface polarization is mainly due to different hierarchical interface structures and heterogeneous structures at the interface surface. The dissipation of EMW within the shielding material is accompanied by various relaxation polarizations, which can be evaluated using the $\varepsilon' - \varepsilon''$ diagram. This diagram is based on the Debye theory and can be simplified using Equation (16).

The response of magnetic media to an electromagnetic field is manifested as magnetic loss, which encompasses hysteresis loss, natural resonance, domain wall resonance, exchange resonance, and eddy current loss. This serves as another key energy dissipation mechanism for EMW absorbers. Domain wall resonance generally occurs in the low-frequency range (1–100 MHz), while magnetic hysteresis loss is typically negligible under weak magnetic fields. When the magnetic field varies near a magnetic material, circulating currents—known as eddy currents—are induced within the material. These eddy currents generate an opposing magnetic field that counteracts the change in the original magnetic field. The interaction between these opposing magnetic fields eventually leads to energy dissipation and the subsequent generation of heat. In the 2–18 GHz frequency range, the formula for eddy current loss (C_0) can be expressed as follows [41–43]:

$$C_0 = \frac{2\pi}{3}\mu_0 \sigma t^2 = \mu''(\mu')^2 f^{-1} \tag{17}$$

where μ_0 and t represent the vacuum conductivity and the diameter of the magnetic particles, respectively. When the frequency varies within the aforementioned range, the eddy current loss remains constant, and it

largely depends on the electrical conductivity, magnetic permeability, and the diameter of the magnetic particles of the material. It is worth noting that when the frequency of the electromagnetic field is in harmony with the rotational motion of the magnetic moment around the equivalent anisotropic field, natural resonance occurs. According to the ferromagnetic principle, the natural resonance frequency governs the magnetic anisotropy of the material, which is commonly referred to as anisotropic energy. The specific relationship is as follows [44,45]:

$$f_r = \frac{\gamma}{2\pi} H_e \tag{18}$$

where f_r represents the self-resonance frequency, γ is the spin magnetic moment ratio, and H_e represents the out-of-plane anisotropic field. Due to the small size effect and confinement effect, the natural resonance frequency increases significantly as the size of the magnetic particles decreases. Furthermore, similar to natural resonance, exchange resonance is also related to the size of the magnetic particles. Surface effects caused by small size also affect the frequency of exchange resonance. The specific equation is as follows [28]:

$$\frac{2\pi f_e}{\gamma} = \frac{C\mu_{kn}^2}{R^2 M_s} + H_0 - \frac{4\pi}{3} M_s + \frac{2K_1}{M_s} \tag{19}$$

where f_e represents the exchange resonance frequency, μ_{kn} is the root of the derivative of the spherical Bessel function, C is the exchange constant, R is the particle radius, M_s is the saturation magnetization, H_0 is the strength of the applied magnetic field, and K_1 is the anisotropy constant of the crystal.

3. Structural Design of the 2D EMW Absorption and Shielding Materials

Due to the unique advantages of 2D materials in the absorption and shielding of EMW, some layered materials have been investigated, such as transition metal carbides, nitrides, or carbon nitrides (MXenes) [46–48], graphene [49–51], transition metal dichalcogenides [52–54], layered double hydroxide [55,56] and *etc*. These materials usually have multiple reflection losses for EMW, and may have some other loss characteristics, such as dielectric loss or magnetic loss. To meet the increasingly high requirements and EMW protection standards at present, many magnetic or conductive materials are applied to prepare composite 2D materials to achieve higher EMW absorption and shielding properties.

In the design of 2D EMW absorption and shielding materials, electrical conductivity serves as the fundamental parameter for achieving high-efficiency shielding performance, as it is essential for inducing EMW reflection. To prevent secondary pollution from reflected EMW, a common strategy is to encapsulate conductive 2D materials with insulating polymers, forming composites with porous structures—such as hybrid matrix films, foams, and aerogel. On the one hand, surfaces rich in pores and with good insulating properties allow EMW to effectively penetrate the material. On the other hand, uniformly dispersed 2D conductive materials can form a hierarchical conductive network, which supports multiple internal reflections of EMW. To ensure that the EMW is absorbed as thoroughly as possible inside the material, the combination of highly dielectric and highly magnetic components is essential. The structural design aligns with contemporary green and sustainable development principles and meets the practical demands of diverse application scenarios. Furthermore, if the 2D materials exhibit high dielectric properties but low electrical conductivity, conductive materials such as MXene or conductive polymers are incorporated to form a continuous conductive network within the composite. In addition, multilayer structures with gradient wave-impedance interfaces can be created by stacking different 2D conductive materials and controlling their interlayer spacing. Compared to the previously mentioned composites, such multilayer designs are not constrained by requirements for uniform dispersion or polymer compatibility, allowing for more precise control over the microstructure and morphology of the 2D materials.

3.1. MXenes

The general formula for MXenes is $M_{n+1}X_n$, where M represents a metal from the early transition metals, X can be carbon, nitrogen, or both, and *n* can be any of the numbers 1, 2, or 3. Generally, the single-element type MXenes without vacancies, such as Mo_2C and Ti_3C_2, are the most common types in previous reports [57–60]. Among them, functionalized $Ti_3C_2T_x$ with variable terminal groups (such as -O, -OH, -F) is a research hotspot in MXene (Figure 2). The core feature of MXene lies in its unique layered structure, adjustable surface chemistry, and excellent electrical conductivity. The material's electrical conductivity contributes to EMW absorption by enhancing dielectric loss, while simultaneously increasing reflection loss, thereby providing effective electromagnetic shielding. The conductivity of MXene ranges from 5 to 2000 S/cm, which completely meets the requirements for high conductivity [61,62].

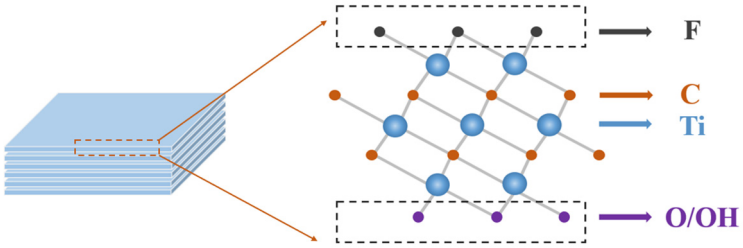

Figure 2. The structural design of MXene ($Ti_3C_2T_x$) with different functional groups.

Malik et al. [63] prepared flexible, cost-effective, and lightweight electromagnetic shielding composites via solution casting. The composites were achieved by incorporating varying loadings of MXene into a 50:50 blend of polyethylene-methyl acrylate (EMA) and ethylene-octene copolymer (EOC). The characterization results showed that even though the MXene was non-uniformly distributed within the polymer and there was no chemical interaction between MXene and the polymer matrix, the composite material still exhibited excellent crystallinity and conductivity. At room temperature, its maximum AC conductivity at 3 GHz was 19.63 S/m with the loading of $Ti_3C_2T_x$ was 15 wt%. This high conductivity resulted in an SE of up to 60.85 dB when the sample thickness was 0.5 μm. However, while high reflectivity brought about high SE, it also caused secondary pollution due to reflected waves. Meanwhile, the direct mixing approach also failed to fully utilize the advantages of the multi-layer structure of MXene.

The multilayer structure of MXene shows a big potential for multiple reflections and absorption of EMW. Therefore, the rational design of the interlayer structure of MXene in the composite material and its uniform dispersion can effectively reflect and absorb EMW multiple times, presenting a better SE. Chen et al. [64] used polymethyl methacrylate (PMMA) microspheres as templates to initially composite with pre-layered MXene through electrostatic assembly, and then prepared three-dimensional lightweight porous $Ti_3C_2T_x$ MXene films by *in-situ* pyrolysis. The experimental results showed that the $Ti_3C_2T_x$ MXene film had excellent electrical conductivity (470 S/m). The $Ti_3C_2T_x$ MXene film exhibited excellent shielding performance in 18–26.5 GHz, with an excellent attenuation of over 60 dB, which was 1.5 times that of the $Ti_3C_2T_x$ sheet under the same conditions. The combined effect of conductive loss, multiple reflection absorption, and interface polarization ensured the EMW shielding performance of the fabricated material. The preparation method solved the problems of stacking and agglomeration of 2D materials, thereby representing a promising, green, environmentally friendly strategy.

In order to further enhance the EMW absorption performance, more complicated structured MXene composites were explored. Zhang et al. [65] combined the MXene layer with three-dimensional (3D) carbon nanotube sponges to fabricate an EMW shielding material with dual control over structure and electromagnetic properties. The different pore diameters on the surface of carbon nanotubes effectively increased the path of EMW incidence and reduced direct reflection. The incident EMW was reflected by

the underlying MXene layer and further attenuated by absorption within the internal structure of the carbon nanotubes. This synergy resulted in a highly effective shielding material characterized by strong absorption and minimal reflection. Performance tests indicated that the composite achieved a SE up to 90 dB at 18 GHz with a reflectivity as low as 0.31—approximately 64% lower than that of the pristine carbon nanotubes. The facts prove that electromagnetic regulation strategy through surface engineering can achieve an enhancement in SE and a reduction in reflectivity without involving complex synthesis processes, which meet the requirements of various intelligent shielding materials for high absorption rate, low reflectivity, and flexible shielding mechanisms. Xiang et al. [66] proposed a new controllable assembly strategy to construct nano/microstructured 2D MXene encapsulated Ni@C layered microcubes (Figure 3), in which they took the self-assembly of 2D metal–organic framework (MOF) templates and the thermal decomposition of electrostatical 2D Ti_3CNT_x thin sheets. Attributed to multi-interface architecture, high defect density, excellent electrical conductivity, notable nuclear magnetic resonance response, and layered porous structure, the prepared composite material achieved outstanding EMW absorption and shielding performance. Experimental results demonstrated that the Ti_3CNT_x/Ni@C composite attained a broad effective absorption bandwidth (EAB) of 5.4 GHz along with strong absorption reaching 65.7 dB. Moreover, the synthesized layered composite exhibited remarkable joule heating capability and multifunctionality, including fire resistance, thermal insulation, and infrared shielding, making it suitable for practical applications in harsh environments.

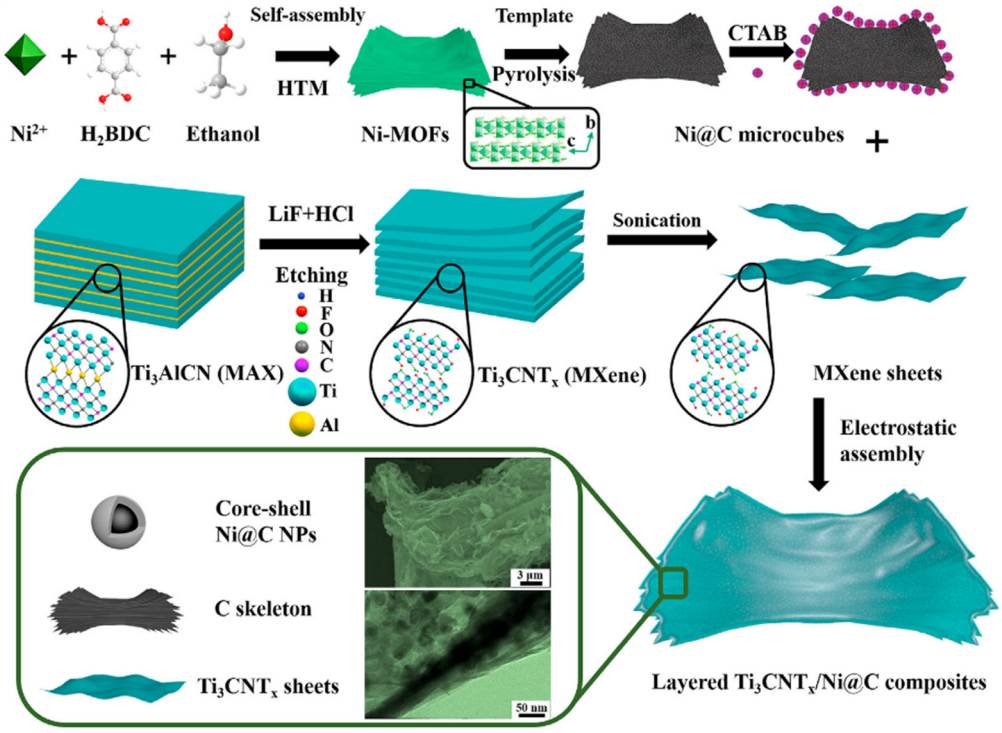

Figure 3. The schematic diagram of the assembly strategy process of layered MXene composite materials. Reproduced with permission of Ref. [66], Copyright 2022 Elsevier.

Besides the structured MXene composites, other composite materials have also been successfully prepared by combining MXene with conductive polymers [61], metal powders [67], ferrites [68] and *etc*. Adding new materials without reducing the conductivity of MXene to enhance the EMW absorption and shielding performance of the raw material, or endowing the raw material with new functions by multifunctional integration, becomes a new and effective approach to meet the current demand for high EMW protection.

3.2. Graphene

Graphene is a nanomaterial with a honeycomb-like hexagonal lattice and hybridized sp^2 orbitals (Figure 4). Due to its high thermal conductivity (5000 W/mK), high electrical conductivity (6000 S/cm), large surface area, and remarkable stability in chemical and thermal environments, graphene has attracted extensive attention in vast fields. Incorporated into polymer composite materials, graphene can be used as an excellent conductive and lightweight material for EMW absorption and shielding [69–71].

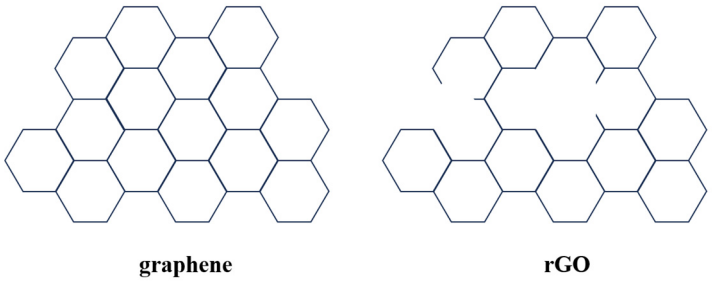

Figure 4. The structure of graphene and rGO single layers.

He et al. [72] demonstrated a green strategy method without solvent melt treatment. By mixing nanofillers to design custom PVDF composite materials, they obtained high EMW SE with low filler loading (Figure 5). The multi-scale structure design utilized the one-dimensional (1D) ballistic electron highway of carbon nanotubes and the 2D charge polarization interface of graphene nanoplates (GnPs). Through a 3D permeable conductive network and a directional heterogeneous interface, they established a dual-phase electromagnetic synergy, achieving multi-scale EMW scattering. The synergistic effect between CNTs and GnPs not only optimized impedance matching but also constructed a continuous conductive network, thereby improving EMW reflection loss. This combination leveraged interface polarization from heterogeneous structures and intrinsic dielectric loss, enabling multiple reflections and absorption of EMW. The resulting PVDF/CNT/GnP ternary composite exhibited a SE of 23.4 dB in the X-band. Similarly, Taymaz et al. [73] prepared 1D CNTs and 2D GNPs-functionalized regenerated cellulose aerogels (RCA) through simple methods such as freezing, solvent exchange, and environmental drying. To improve EMW absorption, a conductive network was set up within the cellulose matrix by capitalizing on the synergistic interaction between CNTs and GnPs. This network induced interface polarization loss due to the conductivity contrast between the conductive network and the cellulose matrix. The prepared hybrid aerogel exhibited a peak SE of 40.2 dB.

Graphene can be converted into reduced graphene oxide (rGO) through chemical oxidation and reduction. The rGO nanosheets possess a large number of lattice defects and oxygen-containing groups, which not only provide good dielectric loss but also can adsorb and fix metal particles to offer additional EMW absorption loss [74,75]. Yao et al. [76] proposed a straightforward strategy for tailoring dielectric and magnetic "genes" to optimize performance in EMWAS and electrochemical lithium storage. The optimized NiO@$NiFe_2O_4$/15rGO composite benefited from its structural and compositional merits, obtaining a SE of 8.69 dB. Moreover, NiO@$NiFe_2O_4$/15rGO demonstrated superior electrochemical lithium storage capability, suggesting its potential for harvesting and storing wasted EMW energy to charge lithium-ion batteries. Yan et al. [77] fabricated a highly conductive nickel foam/wood lignin/rGO dual-network scaffold (LGN) through vacuum-assisted adsorption, freeze-drying, and thermal annealing. Owing to its excellent electrical conductivity (1597.5 S/cm), the PLGN composite got a high SE of 69.9 dB in the frequency range of 8.2–12.4 GHz, indicating strong potential for mitigating electromagnetic interference in electronic devices. High electrical conductivity of GO and the interface polarization of dielectric materials enabled the formed conductive network to have excellent effects on EMW reflection and absorption.

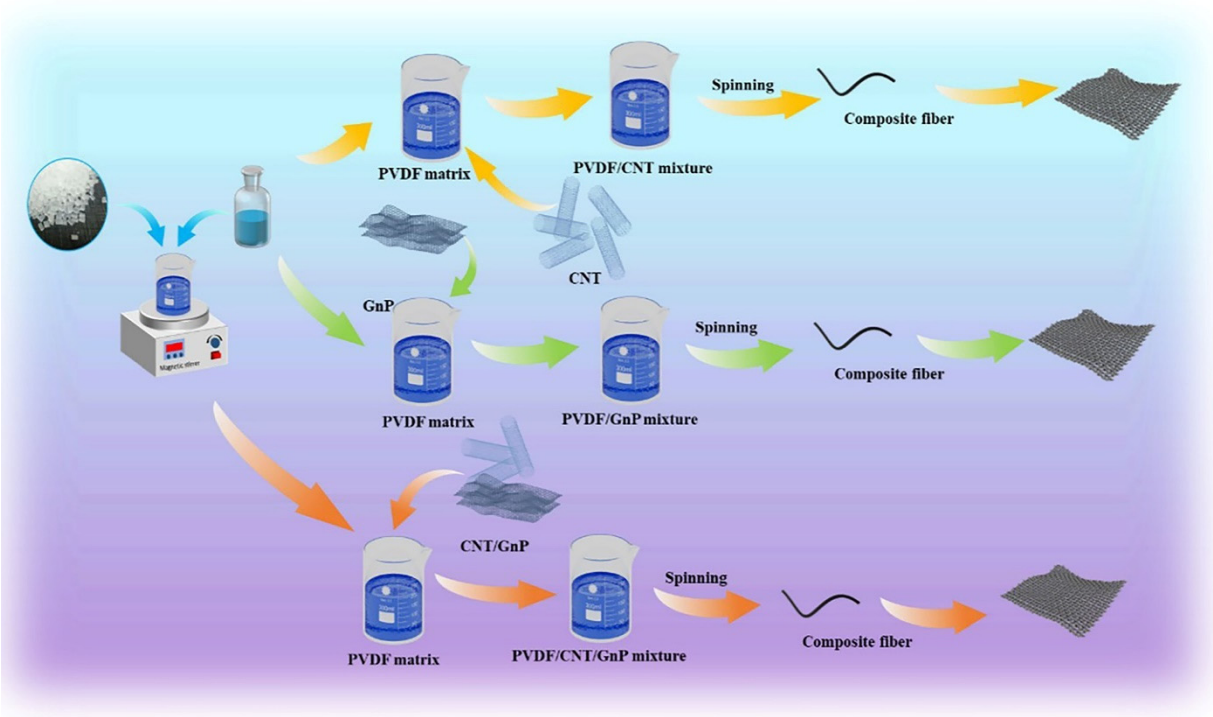

Figure 5. Schematic illustration showing the fabrication process of GO composite materials. Reproduced with permission of Ref. [72], Copyright 2025 The Royal Society of Chemistry.

3.3. Transition Metal Dichalcogenides

Transition metal dichalcogenides (TMDCs), represented by the empirical formula MX_2 (where M = W, Mo, Ti, *etc*.; X = S, Se, Te, *etc*.), constitute a class of emerging materials with diverse application potential (Figure 6). Their typical layered structure, active surface sites, and abundant defects offer a substantial chance for polarization effects. Recently, TMDCs have gained much attention as promising EMW absorption and shielding materials [78–80].

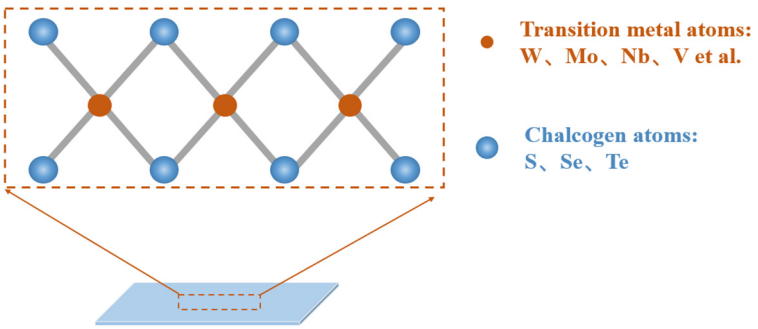

Figure 6. The structure and composition of the TMDCs single-layer.

Sharma et al. [81] utilized a unique method of water vapor-induced phase separation to fabricate a microporous structure of layered rGO/molybdenum disulfide reinforced TPU foam. Their results showed that the total SE of the 7 wt% rGO/MoS_2/TPU foam was 32 dB. The foam material's layered heterogeneous structure promoted the formation of electric dipoles and facilitated efficient carrier hopping. Combined with the multiple internal reflections induced by its micro-porous architecture, the prepared foam achieved a maximum wave attenuation of 99.9% and a significant absorption-dominated shielding contribution, accounting for 92% of the total SE. Zhu et al. [82] successfully synthesized a multifunctional WSe_2/Co_3C composite material with a multi-dimensional structure through the hydrothermal method. The prepared

material exhibited excellent electromagnetic properties with a rich electromagnetic response mechanism. Benefiting from the synergistic contribution of dielectric and magnetic losses, the WSe_2/Co_3C composite displayed outstanding EMW SE, obtaining an average SE of 28.97 dB, which accounted for approximately 70% of its total attenuation. The SE_A contributed over 80% of the SE, significantly reducing the reflection of electromagnetic waves. Ghosh et al. [83] explored a cross-dimensional composite system composed of dielectric phase and magnetic phase (WS_2/dual-phase lithium iron oxide) for EMW shielding applications. WS_2, a 2D material with distinctive dielectric properties and sheet-like morphology, exhibited a pronounced surface effect. In contrast, the dual-phase lithium iron oxide nanocomposite possessed a crystalline structure and higher magnetic loss. Incorporating WS_2 into the dual-phase lithium iron oxide markedly enhanced the overall SE of the nanocomposite. Results indicated that the composite held a maximum SE of 55.6 dB at 12.4 GHz.

3.4. Layered Double Hydroxide

Layered double hydroxide (LDH) is a new type of 2D inorganic layered nanomaterial, which is a natural or artificially synthesized anionic clay. Its general formula is $[M^{II}_{1-x}\ M^{III}_x\ (OH)_2]^{x+}\ (A^{n-})_{x/n}\cdot yH_2O$, where M^{II} and M^{III} represent divalent and trivalent ions, respectively, A^{n-} denotes an anion, and x corresponds to the molar ratio $M^{III}/(M^{II}+M^{III})$ (Figure 7). LDHs take advantage of high quality, low cost, good thermal stability, and environmental friendliness. LDH is widely used in many fields such as adsorption, catalysis, and stabilizers. In addition, the unique layered structure of hydrotalcite easily forms multiple interfaces, which can obviously enhance the loss of EMW [84–86].

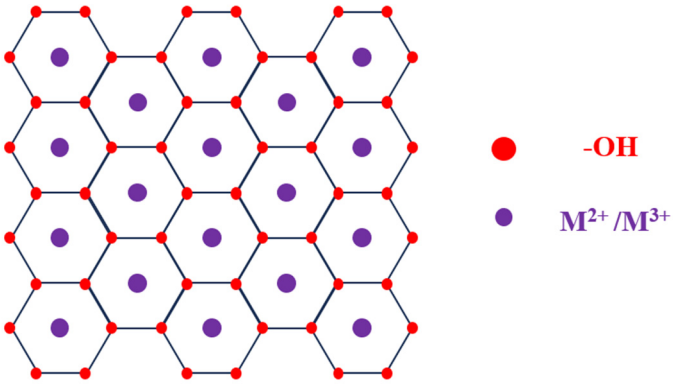

Figure 7. The structure and component composition of the LDH mainboard layer.

Lyu et al. [87] developed a multifunctional cotton fabric (PPy/NiCoAl-LDH/cotton) with a layered array architecture. They initially grew NiCoAl-layered double hydroxide (NiCoAl-LDH) nanosheet arrays on cotton fibers, and subsequently conducted *in-situ* polymerization to deposit a continuous and dense conductive polypyrrole (PPy) layer. The resulting fabric exhibited excellent SE of 38.83 dB, as well as notable flexibility and durability. Duan et al. [88] took *in situ* growth of LDH on the surface of MXene through electrostatic self-assembly, resulting in an approximately 5 μm-diameter ball-shaped intermediate product (LDH@MXene). The prepared LDH@MXeneHT500 material showed soft magnetic behavior, which promoted the transport of induced charges and facilitated the dissipation of electromagnetic energy. As a result, the LDH@MXeneHT500 nanohybrid obtained a high SE of 47.2 dB in the X-band. To extend its applicability, a polydimethylsiloxane (PDMS)/LDH@MXeneHT500 nanocomposite was further developed. The composite demonstrated improved mechanical strength (9.48 MPa) and effective electromagnetic protection, sustaining an electromagnetic wave shielding effectiveness above 50 dB over the 3–18 GHz frequency range.

3.5. Others

In addition to the materials mentioned above that are widely used, some other two-dimensional materials have also been employed in the fields of electromagnetic wave absorption and shielding, such as black phosphorus [89], hexagonal boron nitride [90–93], 2D-MOF [94–97], *etc*. The relevant data from reports in the literature are listed in Table 1. The respective characteristics of different materials and their approaches in the structural design of composite materials are presented (Table 1). Artificially synthesized two-dimensional materials have demonstrated excellent performance in the field of electromagnetic wave protection [98–102]. In some cases, the complex preparation methods, high cost of raw materials, and the significant environmental impact of solvent use may have significant impacts on industrial applications [103–107]. Research is now increasingly focused on developing alternative, low-cost raw materials and greener synthesis routes.

Table 1. The shielding performances of typical 2D EMW absorption and shielding materials.

2D Materials	Sample	Structure	Frequency Range (GHz)	SE (dB)	Other Functions	Refs.
MXene	EMA/EOC/$Ti_3C_2T_x$	Film	2–4	60.8	Lightweight	[63]
	$Ti_3C_2T_x$ MXene@PMMA	3D film	18–26.5	60.3	Lightweight	[64]
	CNTS/MXene	Sponge	8–12	80	/	[65]
	$Ti_3C_2T_x$/Ni@C	Multilayer	8–12	66.7	Flame-retardant	[66]
	SMPU-MXene/AgNWs	Membrane	8–12	60	Infrared stealth	[108]
	AgNW/MXene	Film	8–20	60.2	High mechanical strength	[109]
	PVDF/SiCnw/MXene	Foam	12.4–18	32.6	Lightweight	[110]
	MXene($Ti_3C_2T_x$)/ANFs	Aerogel	8.2–12.4	56.8	High mechanical strength	[111]
Graphene	PVDF/CNT/GnP	Film	18–26.5	23.4	Extreme flexibility	[72]
	C7G7	Aerogel	8.2–12.4	20	Lightweight	[73]
	NiO@$NiFe_2O_4$/15rGO	Multilayer	2–18	8.7	Energy storage	[76]
	PEG/Ni–F/LN-rGO	Foam	8.2–12.4	69.9	Superior light absorption	[77]
	EP/AgNW/TAGA	Aerogel	8.2–12.4	84	High mechanical strength	[112]
	graphene/AgNWs	Multilayer	8.2–12.4	76.6	/	[113]
	Ag/rGO-AF/rGO-F/PDMS	Aerogel- Foam	8.2–12.4	68.9	/	[114]
	MS A1000	Aerogel	8.2–12.4	55.8	High mechanical strength	[115]
	RGO/CNT@Epoxy/AgNW	Film	8.2–12.5	40	/	[116]
TMDCs	rGO/MoS_2/TPU	Foam	8.2–12.4	32	High mechanical strength	[81]
	WSe_2/Co_3C	Multilayer	8.2–12.4	29	/	[82]
	W(33)L(67)	Multilayer	8.2–12.4	55.6	/	[83]
LDH	PPy/NiCoAl-LDH/Cotton	Cotton fabric	8.2–12.4	38.8	Photothermal conversion	[87]
	LDH@$MXene_{HT500}$	Multilayer	3–18	50	High mechanical strength	[88]
	APP@CoAl-LDH@Si	Film	8.2–12.4	43.6	Flame-retardant	[117]
	CM_3HTA	Film	8.2–12.4	43.5	Flame-retardant	[118]
	PILs/MOF-LDH-Zr	Fibers	8.2–12.5	58	High mechanical strength	[119]
	MLPC	Film	8.2–12.4	30	High mechanical strength	[120]
	LZCFM	Foam	8.2–12.4	43.9	High thermal stability	[121]
	PILs/MOF-LDH-Zr	Leather	8.2–12.4	32.3	Flexibility	[122]
Black phosphorene	CMB	Film	8.2–12.4	58	Flame-retardant	[123]
	M-B-M(Ni)	Film	8.2–12.4	50	Infrared stealth	[124]
2D-MOF	CoFe/CoCu-PCFs	Film	2–18	73.5	Flexibility	[125]
	CoNPs/NrGO	Film	8.2–12.4	33.5	High mechanical strength	[126]
Hexagonal boron nitride	$M_{20}PPFB_6$	Multilayer	8.2–12.4	58.1	Remarkable stability	[127]
	PCM	Cotton	8.2–12.4	23.4	Thermal regulation	[128]
	Ag@BN/BN/PEI	Multilayer	8.2–12.4	24	/	[129]

h-BN/SCG/quartz/Ag	Film	8–12	28.8	Long-term stability	[130]
TIMs	Multilayer	8.2–12.4	29	Flame-retardant	[131]

4. 2D Natural Mineral-Based EMW Absorption and Shielding Materials

Mineral-based EMW absorption and shielding materials have emerged as a research focus in EMW protection, owing to their outstanding EMW absorption and shielding performance, robust mechanical properties, and strong thermal and oxidation resistance. Among them, 2D natural mineral materials like montmorillonite (MMT), graphite, talc, mica, and hydrotalcite have unique advantages in this field due to their highly adjustable electromagnetic parameters. Surprisingly, they can precisely control impedance matching through structural design. This characteristic enables the mineral-based materials to take "low reflection and high absorption" effects over a wide frequency range. Once electromagnetic waves enter the material, they will be converted into heat energy through mechanisms such as dielectric loss (such as interface polarization, dipole relaxation) and magnetic loss (such as natural resonance, eddy current effect), which is crucial for applications that require eliminating electromagnetic waves, such as radar stealth and electromagnetic compatibility [132]. In addition, the layered structure of 2D mineral materials provides them with unique advantages in EMW absorption and shielding. By taking advantage of the layered properties of natural minerals, they can even be separated into 2D sheets through physical or chemical methods. The sheet structure can increase the propagation path of EMW within the material, allowing them to be reflected and absorbed multiple times, thereby greatly enhancing the shielding effect.

Compared with traditional metal-based or carbon-based materials, these 2D layered structures derived from natural minerals not only possess low density, high flexibility, and good processing adaptability, but also can achieve efficient attenuation, multiple scattering, and loss conversion of EMW through nano-scale structural design (such as layer-by-layer assembly, intercalation composite, construction of three-dimensional networks, *etc*.) in coordination. Although natural minerals are widely available, their inherent properties may not be sufficient to meet the demands of high-end applications, so functional modification is required.

Through the direct carbonization method, Wang et al. [133] prepared a phenolic resin-based carbon foam composite material with a hierarchical porous structure for the first time by combining carbon nanotubes and 2D montmorillonite (MMT) as multi-scale reinforcing agents with hollow microspheres. The composite material (5 wt.% MMT) exhibited remarkable characteristics of multifunctional synergistic strengthening. Its compressive strength reached 8.54 MPa, which was 116% higher than that of pure carbon foam. The SE at the X-band was as high as 65 dB, and the shielding mechanism was mainly absorption. The prepared material integrated high strength, high electromagnetic shielding, and good heat insulation, making it an ideal multifunctional material for thermal protection. Dang et al. [134] employed an alternating vacuum-assisted filtration (VAF) process to fabricate a multifunctional 2D MMT/aramid nanofibers@MXene (MMT/ANFs@MXene) nanocomposite with an alternating multilayer architecture (Figure 8). They designed a structure where the "MXene layer (conductive layer)" and the "AT layer (ANFs/MMT, mechanical reinforcement and insulation protection layer)" were alternately superimposed. The prepared composite material had high mechanical strength (tensile strength of 154.66 MPa, strain of 14.22%), excellent EMI SE (58.4 dB), as well as strong fire-resistant protection performance. Even after burning for 30 s, it still maintained an SE of approximately 34 dB. Generally, structural design with precise functional modification can collaboratively optimize the mechanical, electromagnetic shielding, joule heating, and flame retardant properties within a single system.

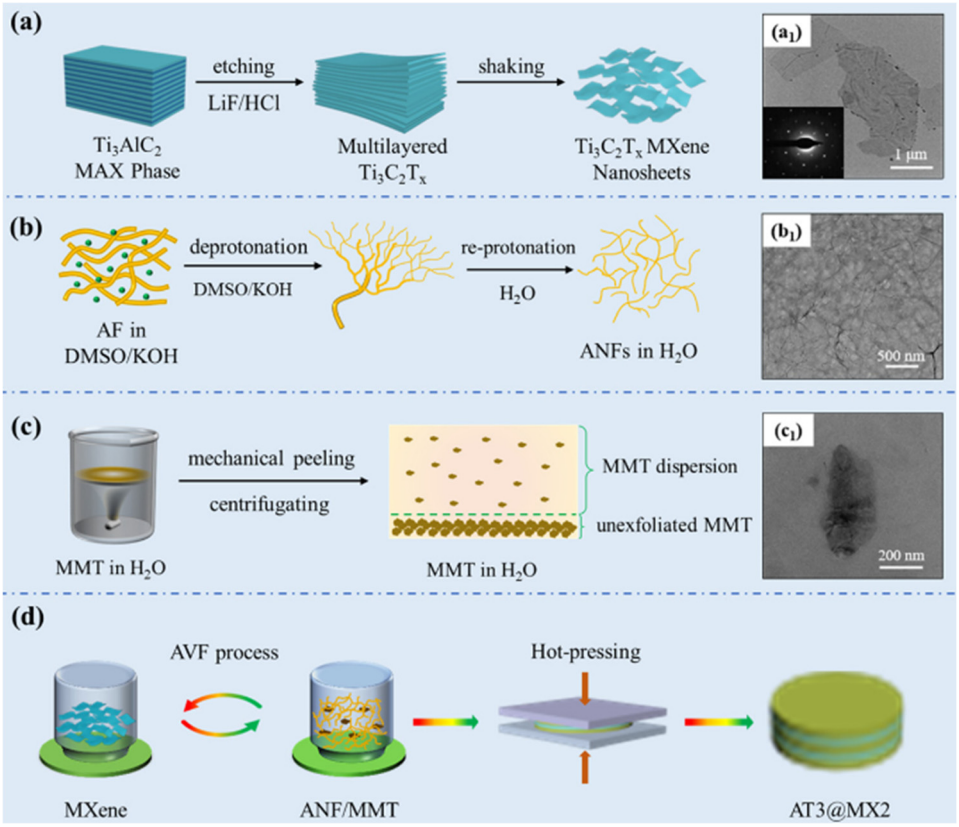

Figure 8. Schematic illustration of the fabrication process of montmorillonite composite materials, showing (**a**–**d**) $Ti_3C_2T_x$ MXene nanosheets, MMT, ANFs and MMT/ANFs@MXene nanocomposite. Reproduced with permission of Ref. [134], Copyright 2022 The Royal Society of Chemistry.

Jiang et al. [135] employed a simple, green, and cost-effective mechanical mixing heating compression molding method to initially prepare a 2D natural graphite/UHMWPE EMW shielding composite material with a typical "isolation structure". This process did not need high-strength dispersion or any organic solvents. Graphite particles were selectively distributed on the polymer polyhedral interfaces, thereby constructing an efficient isolation structure conductive network. The product achieved an outstanding SE of up to 51.6 dB even with a low graphite content. Its electromagnetic shielding mechanism was mainly based on absorption. Importantly, the uniqueness of this research lies in the successful production of high-performance electromagnetic shielding material using inexpensive micron-sized natural graphite through structural design rather than increasing the filler dosage. The progress may open up more new routes for the effective utilization of economical fillers in functional composite materials.

In recently years, more and more 2D mineral materials have been explored to create mineral-based EMW absorption and shieldingmaterials for the absorption and shielding of electromagnetic waves. Table 2 lists the shielding performances of several typical 2D mineral-based EMW absorption and shielding materials. It can be seen from the table that the combination of mineral materials with magnetic or conductive materials is currently a research trend. Moreover, most composite materials possess additional functionalities such as flame retardancy and high strength, and there is a growing tendency towards multifunctional integration, which is very important for the future development of highly efficient EMW absorption and shielding.

Table 2. The shielding performances of several typical 2D mineral-based EMW absorption and shielding materials.

Mineral	Single-Layer Structure	Sample	Frequency Range (GHz)	SE	Other Functions	Refs.
montmorillonite	$(Ca,Na)_x[(Al,Mg)_2(Si_4O_{10})(OH)_2]\cdot nH_2O$	CNT/MMT	8.2–12.4	65 dB	Heat insulation performance	[133]
montmorillonite	$(Ca,Na)_x[(Al,Mg)_2(Si_4O_{10})(OH)_2]\cdot nH_2O$	MMT/ANFs@MXene	8.2–12.4	58.4 dB	High mechanical strength, thermal conductivity and flame retardancy	[134]
montmorillonite	$(Ca,Na)_x[(Al,Mg)_2(Si_4O_{10})(OH)_2]\cdot nH_2O$	CMMPs	8.2–12.4	56.1 dB	High mechanical strength and fire resistance	[136]
natural graphite	C	Graphite/UHMWPE	8.2–12.4	51.6 dB	/	[135]
natural microcrystalline graphite	C	MG@SiC-NWs	13.4–18	42.94 dB	/	[137]
talc	$Mg_3(Si_4O_{10})(OH)_2$	MAS glass–ceramic	12.4–15	6 dB	/	[138]
mica	SiO_2	EVA/GP/MP/OMMT/SCF	8.2–12.4	36 dB	High temperature resistance	[139]
hydrotalcite	$Mg_6Al_2(OH)_{16}CO_3\cdot 4H_2O$	rigid foam composites	0.6–2.5	45 dB	Sound absorption and heat insulation properties	[140]

5. The Application of 2D EMW Absorption and Shielding Materials

To ensure electromagnetic compatibility and information security, 2D EMW absorption and shielding materials, as the key functional materials, are critical in multiple cutting-edge fields with strict requirements for the electromagnetic environment, such as electronic and electrical equipment, aerospace, medical treatment and health, personal protection, and military defense. Among all the aforementioned areas, the military and defense sector has the most stringent requirements for shielding performance, which not only aims at high SE across a wide frequency band, but also needs to consider aspects such as stealth, radiation resistance, extreme environment adaptation, and multifunctional integration [138,141]. It is the core driving force and verification platform for promoting 2D microwave shielding materials towards high performance, lightweight, and intelligent directions, and holds crucial strategic significance.

5.1. Electronic and Electrical Equipment

In the field of electronic and electrical equipment, the issue of electromagnetic compatibility (EMC) has become increasingly prominent. 2D shielding materials, with their flexible controllable electromagnetic properties and adaptable structural designs, perfectly match the development needs of modern electronic devices for integration and miniaturization. These materials are mainly used to protect the internal precision electronic components of the equipment from external EMW. They can effectively suppress the electromagnetic radiation and leakage generated by the equipment during operation, and ensure the quality of signal transmission and the stability of system operation.

Lu et al. [142] adopted a method combining mechanical mixing with subsequent chain extension to prepare a series of environmentally friendly and renewable water-based polyurethane (ADWPU)/2D MXene composite films based on castor oil used for EMW protection products. They mixed MXene nanosheets with WPU emulsion containing dynamic and reversible disulfide covalent bonds, constructing a controllable, similar to isolation, and conductive network within the material to protect the internal materials from EMW interference. Due to the disulfide exchange effect, the composite material obtained a mechanical strength of 15 MPa even when the elongation at break is relatively low, and it possessed self-

repairing and shape-memory properties. Zhao et al. [143] uniformly fixed high-purity 1T phase 2D MoS_2 petals on the wrinkled surface of rGO, successfully synthesizing 1T-MoS_2@N-rGO nanocomposite. It effectively optimized impedance matching by fixing the 1T-MoS_2 petals and synergized multiple EMW attenuation mechanisms, thereby achieving "thin, wide, and strong" high-performance absorption. These characteristics are capable of meeting the demands of highly flexible and lightweight products.

5.2. Personal Protection

In the field of personal protective, the increasingly complex electromagnetic radiation environment demands efficient electromagnetic shielding. Electromagnetic radiation may pose potential hazards to human health. Therefore, designs of new shielding materials are optimizing the fillers and innovating the structures to provide technical paths for protective equipment, which combine high performance with wearability to ensure the safety of personnel.

Xiang et al. [144] used the electrostatic self-assembly method to embed the 1D CNTs/Co nanocomposite in the form of a sea urchin shape into the 2D $Ti_3C_2T_x$ MXene layer, successfully preparing $Ti_3C_2T_x$/CNT/Co cobalt nanocomposite with a 2D/1D/nanodimensional hierarchical structure. The polydimethylsiloxane thin layer forms a hydrophilic layered $Ti_3C_2T_x$/CNTs/Co hydrophobic structure, which prevented the degradation/oxidation of MXene under high humidity conditions. Moreover, the $Ti_3C_2T_x$/CNTs/Co film exhibited excellent photothermal conversion performance, with high thermal cycling stability and sustainability. Zhang et al. [145] employed electrospinning technology to load zero-dimensional $Fe_{0.64}Ni_{0.36}$ magnetic nanoparticles onto 2D MXene nanosheets and simultaneously embed them into 1D carbon nanofibers, thereby constructing a novel $Fe_{0.64}Ni_{0.36}$/MXene/CNFs flexible nanofiber membrane with a multi-component heterogeneous structure network. As a result, this electromagnetic protection fabric not only exhibited outstanding radiation-shielding performance but also possessed high flexibility, hydrophobicity, and low density. These are indispensable elements for improving personal protective measures.

5.3. Aerospace

Aerospace vehicles have extremely strict requirements for the properties of materials. They must possess characteristics such as "lightweight, high strength, resistance to extreme environments, and multi-functionality". 2D natural mineral materials, with their inherent lightweight properties and the advantage of functional design, can precisely meet these challenges. These materials are mainly used in aircraft to protect sensitive avionics systems and may be used for functions such as stealth or thermal management.

Fan et al. [146] employed a straightforward strategy of integrating highly conductive 2D $Ti_3C_2T_x$ MXene nanosheets with GO, successfully fabricating a highly conductive MXene/GO composite foam via freeze-drying and heat treatment. Based on a 3D network structure with low density and high porosity, by taking advantage of its high conductivity and the internally connected porous structure, it promoted the effective attenuation of EMW and realized a perfect combination of lightweight, high conductivity, and high specific shielding efficiency. As noticed, this kind of highly promising EMW shielding material holds broad application potential in aerospace. Zhang et al. [147] successfully synthesized a CoNi@$Ti_3C_2T_x$ MXene composite material with a 0D/2D hybrid structure by depositing CoNi nanoparticles on both sides of MXene through the hydrothermal method. Combined with the unique 0D/2D structure, enhanced interface polarization, magnetic coupling effect, and multiple scattering mechanism, the prepared material obtained outstanding comprehensive performance, namely "strong absorption, wide bandwidth, and moderate thickness". The lightweight and high-strength materials effectively reduced the design difficulty of the new generation of aircraft, making them a hot topic of current research.

5.4. Medical Treatment and Health

As for medical treatment and health, the application of EMW absorption and shielding materials mainly focuses on two aspects: one is to protect highly precise medical diagnostic equipment (such as MRI and CT) from external electromagnetic noise, ensuring imaging quality; the other is to protect the human body or specific medical environments, reducing the potential impact of electromagnetic radiation. Due to the characteristics of certain natural clay minerals and their ability to be processed into flexible films, they demonstrate great potential in this field. Through functionalization design, these materials can be made into flexible shielding fabrics, shielding coatings, or shielding room materials, achieving local or overall electromagnetic protection while ensuring safety and comfort.

Antonez et al. [148] employed a unique polishing technique to cut, bond, and finely polish the 2D natural shungite stone (a type of shale rich in GO) rock, and then fabricated ultra-thin flexible GO-rich shale shielding plates with a thickness of only 10 to 20 μm. The most outstanding feature of this material was that it integrated the natural structure, ultra-thin thickness, excellent flexibility, and outstanding comprehensive shielding performance (combining efficient reflection and absorption capabilities) into one, demonstrating great potential as a green, low-cost, and durable next-generation flexible electromagnetic protection coating. Liu et al. [149] adopted a collaborative strategy of integrating in-situ growth, vacuum-assisted filtration, and self-reduction to successfully prepare a multi-level hierarchical structure composed of Fe_3O_4-Fe nanoparticles/carbon nanofibers/2D aluminum-Fe_3O_4-Fe nanosheets composite materials. The multi-level hierarchical structure design enabled the integration of the material's multiple functions and the exertion of their respective effects, which was beneficial for the precision instruments and the protection of human health.

5.5. Military Defense

In military defense, the control of EMW is one of the core capabilities, involving multiple key aspects such as stealth, anti-interference, and information security. Through specific functionalization and structural design, 2D materials can be utilized to develop new-generation wide-band, lightweight, and weather-resistant stealth coatings, camouflage nets, or electromagnetic shielding compartments for military equipment, thereby enhancing the survival capabilities and combat effectiveness of weapons and equipment.

Shan et al. [150] prepared three 2D MOF materials with inherent electrical conductivity, $M_3(HHTP)_2$ (where M = copper, zinc, and nickel). Among them, $Cu_3(HHTP)_2$, which had higher electron conductivity and a hexagonal prism rod-like morphology, exhibited the best performance. Under a matching thickness of 2.1 mm, its minimum reflection loss reached −56.45 dB, with an EAB of up to 5.76 GHz, covering the entire Ku band and having potential applications in the military field. Wu et al. [151] successfully prepared 2D MoS_2/CoNi heterojunction composite materials by combining the ion insertion technique with the simple hydrothermal method. The minimum RL of all samples was lower than −50 dB. This composite material achieved impedance matching through the cooperative construction of the heterojunction and simultaneously enhanced multiple loss mechanisms. These progresses provide a highly promising technical path for the development of low-cost, customizable, lightweight, and broadband absorbing materials, especially for the design of protective materials for high-tech weapons.

6. Summary and Outlook

Owing to their distinctive layered structure, abundant surface functional groups, and high specific surface area, 2D materials have been successfully employed in EMW absorption and shielding applications. This review elaborates on the fundamental mechanism and material structure aspects that explain why 2D materials can significantly enhance the attenuation of EMW. Existing practices have shown that the multiple reflection losses of the multi-layer structure require the combined effect of reflection by conductive

materials and absorption by dielectric materials. Consequently, combining multiple materials has become a prominent research focus in the field of 2D materials. In material design, a porous surface is essential to reduce the direct reflection of EMW and enhance their absorption. The porous structure can trap incident EMW within the material, thereby preventing their secondary pollution. Moreover, the high conductivity of the material should be concentrated in the interior and the bottom to prevent direct reflection while increasing the conductive loss of electromagnetic waves. Meanwhile, the high conductivity of the material greatly enhances the multiple internal reflections of EMW. Most importantly, the interface polarization loss generated at the interfaces of the 2D material and its internal defects, as well as the polarization loss arising from the integration of magnetic or conductive components, constitute the key mechanisms for EMW absorption. The combination of 2D multiple reflections and absorption can achieve a high absorption rate and a high SE for EMW, and also enable efficient conversion of energy.

Although encouraging progress has been made in the development of 2D electronic-warfare protection materials, the following aspects for further research are still required to accelerate and expand the application of EMW absorption and shielding technology.

(1) Precise design and synthesis. The precise design and synthesis of target composites for highly efficient EMW absorption and shielding based on 2D materials still face some big challenges. How to precisely design the structure of materials from both microscopic and macroscopic perspectives to achieve graded protection against EMW frequencies and wide-band protection requires more investigation. At the microscopic level, to achieve 'on-demand tailoring' of the permittivity and magnetic permeability, it is necessary to focus on the influence of factors such as crystal structure, crystal defects, dopant atoms, and hetero-interface on the intrinsic electromagnetic parameters of materials. At the macro level, the agglomeration and stacking of the lamellar materials, as well as the weak bonding forces at the interfaces, are crucial problems to solve, which determine the material's ability to exhibit high EMW protection performance. Future efforts should focus on targeted functionalization at specific active sites of 2D materials, enabling precise modification and grafting. By initiating from the controlled layer-by-layer exfoliation of 2D materials, precise tuning of interlayer spacing will be realized.

(2) Multifunctional integration. Currently, the requirements for EMW absorption and shielding materials are not limited to enhancing electromagnetic protection performance, but rather focus on integrating multiple functions into a single comprehensive composite material. Moreover, the requirements for functions vary across different fields of application. There are many other demands for EMW absorption and shielding products such as flame retardancy and lightweight yet high-strength properties in aerospace, tolerance to extreme environments in national defense, flexibility, comfort and low toxicity in personal protection. These requirements for functionality are pushing the structural design and multifunctional integration to a new level. More attention should be paid on developing new materials with diverse functional properties, investigating their potential for synergistic combination and integration; exploring novel modification and composite strategies, and investigating the multifunctional characteristics of multi-dimensional composite materials.

(3) Green and sustainable synthetic process. To meet the higher application requirements for energy conservation across diverse fields, the selection of materials and the preparation process should be green and sustainable. Low-cost, green, and natural mineral materials are inevitably the focus of research. Combining green production technologies with low-energy consumption processes is a necessary requirement for future development. How to obtain a more efficient, high-value product with considerable economic benefits lies in developing more green and sustainable synthetic strategies.

Acknowledgments

The research group leader wants to extend its appreciation to its members for their resilience and dedication during this review.

Author Contributions

The manuscript "Structural Design and Application of Two-Dimensional Electromagnetic Wave Absorption and Shielding Materials" is for consideration in Sustainable Polymer & Energy by the following authors: C.L., Q.L., L.X., Z.F., Q.M. and G.Z., with the following individual contributions. G.Z. proposes the outline and the main structure of the paper. C.L. and Q.L. were responsible for formalization, collection and analysis of data. L.X. and Z.F. were responsible for interpreting and reviewing the data collected. Q.M. and G.Z. were responsible for supervising, overseeing and reviewing the complete manuscript.

Ethics Statement

No ethical approval is needed, as no humans and animals are involved.

Informed Consent Statement

Not applicable.

Data Availability Statement

Data sharing is not applicable to this article, as no new data were created in this study.

Funding

This work was partly supported by Research and Development Program of Zhejiang Provincial Bureau of Science and Technology, China (Grants No. 2021C03169).

Declaration of Competing Interest

The authors declare that they have no known competing financial interests or personal relationships that could have appeared to influence the work reported in this paper.

References

1. Wang Y, Zhong Y, Kang J, Zhang B, Ma Z, Zhao Q, et al. Multifunctional rigid polyimide foams with outstanding EMI shielding and wave absorption via densification strategy. *J. Mater. Sci. Technol.* **2025**, *227*, 155–163. DOI:10.1016/j.jmst.2024.12.021
2. Zhao W, Dong J, Li Z, Zhou B, Liu C, Feng Y. Centrifugal inertia-induced directional alignment of AgNW network for preparing transparent electromagnetic interference shielding films with joule heating ability. *Adv. Sci.* **2024**, *11*, 2406758. DOI:10.1002/advs.202406758
3. Li S, Sun Y, Meng F, Jiang X, Yu H. Lightweight Fe_3O_4/Fe/C/rGO multifunctional aerogel for efficient microwave absorption, electromagnetic interference shielding, hydrophobicity and thermal insulation. *Chem. Eng. J.* **2024**, *498*, 155405. DOI:10.1016/j.cej.2024.155405
4. Zhou YJ, Wu XB, Cai XD, Xu HX, Li QY, Xiong W, et al. Smart meta-device powered by stray microwave energies: A green approach to shielding external interference and detection. *Appl. Energy* **2025**, *378*, 124770. DOI:10.1016/j.apenergy.2024.124770
5. Ruan J, Chang Z, Rong H, Alomar TS, Zhu D, AlMasoud N, et al. High-conductivity nickel shells encapsulated wood-derived porous carbon for improved electromagnetic interference shielding. *Carbon* **2023**, *213*, 118208. DOI:10.1016/j.carbon.2023.118208

6. Dogari H, Ghafuri H, Peymanfar R. Ultrathin microwave absorbing structures at the K-band from PDA-implanted CNTs, doped conjugated carbon using peganum harmala seeds and turpentine derivatives. *Adv. Sustain. Syst.* **2025**, *9*, 2400793. DOI:10.1002/adsu.202400793
7. Akram S, Ashraf M, Javid A, Abid HA, Ahmad S, Nawab Y, et al. Recent advances in electromagnetic interference (EMI) shielding textiles: A comprehensive review. *Synth. Met.* **2023**, *294*, 117305. DOI:10.1016/j.synthmet.2023.117305
8. Nan Z, Wei W, Lin Z, Chang J, Hao Y. Flexible nanocomposite conductors for electromagnetic interference shielding. *Nano-Micro Lett.* **2023**, *15,* 172. DOI:10.1007/s40820-023-01122-5
9. Gao X, Wang X, Cai J, Zhang Y, Zhang J, Bi S, et al. CNT cluster arrays grown on carbon fiber for excellent green EMI shielding and microwave absorbing. *Carbon* **2023**, *211*, 118083. DOI:10.1016/j.carbon.2023.118083
10. Huang L, He Y, Gao Z, Du H, Zhang R, Zhang L, et al. Hybrid-structured carbon fiber fabric/silk fiber non-woven fabric/carbonyl iron powder/epoxy composites with highly efficient electromagnetic interference shielding and mechanical properties. *Compos. Sci Technol.* **2024**, *258*, 110868. DOI:10.1016/j.compscitech.2024.110868
11. Nguyen QD, Choi CG. Recent advances in multifunctional electromagnetic interference shielding materials. *Heliyon* **2024**, *10*, e31118. DOI:10.1016/j.heliyon.2024.e31118
12. Yadav RS, Kuřitka I. Recent developments on nanocomposites based on spinel ferrite and carbon nanotubes for applications in electromagnetic interference shielding and microwave absorption. *Crit. Rev. Solid State* **2024**, *49*, 371–407. DOI:10.1080/10408436.2023.2214577
13. Liu JT, Zheng YC, Hou X, Feng XR, Jiang K, Wang M. Structured carbon for electromagnetic shielding and microwave absorption from carbonization of waste polymer: A review. *Chem. Eng. J.* **2024**, *496*, 154013. DOI:10.1016/j.cej.2024.154013
14. Zheng J, Hang T, Sun Z, Jiang S, Li Z, Dong W, et al. Temperature-stimulated composite foams for reversibly switching microwave absorption towards electromagnetic interference shielding capability. *Diam. Relat. Mater.* **2023**, *140*, 110499. DOI:10.1016/j.diamond.2023.110499
15. Hou X, Feng XR, Jiang K, Zheng YC, Liu JT, Wang M. Recent progress in smart electromagnetic interference shielding materials. *J. Mater. Sci. Technol.* **2024**, *186*, 256–271. DOI:10.1016/j.jmst.2024.01.008
16. Tiwari A, Tiwari A, Bhatia A, Chadha U, Kandregula S, Selvaraj SK, et al. Nanomaterials for electromagnetic interference shielding applications: A review. *Nano* **2022**, *17*, 2230001. DOI:10.1142/S1793292022300018
17. Zhang G, Wang H, Xie W, Zhou S, Nie Z, Niwamanya G, et al. Advancements in 3D-printed architectures for electromagnetic interference shields. *J. Mater. Chem. A* **2024**, *12*, 5581–5605. DOI:10.1039/D3TA07181B
18. Qin L, Gao M, Zhang M, Li X, Ru R, Zhang GL, et al. Bioinspired assembly of double honeycomb-like hierarchical capsule confined encapsulation with functional micro/nanocrystals. *Small* **2020**, *16*, 2004692. DOI:10.1002/smll.202004692
19. Zhou M, Yu Z, Yan Q, Zhang X. Asymmetric structural design for absorption-dominated electromagnetic interference shielding composites. *Adv. Funct. Mater.* **2025**, *35*, 2423884. DOI:10.1002/adfm.202423884
20. Wang YY, Zhang F, Li N, Shi JF, Jia LC, Yan DX, et al. Carbon-based aerogels and foams for electromagnetic interference shielding: A review. *Carbon* **2023**, *205*, 10–26. DOI:10.1016/j.carbon.2023.01.007
21. Li P, Wang H, Ju Z, Jin Z, Ma J, Yang L, et al. $Ti_3C_2T_x$ MXene- and sulfuric acid-treated double-network hydrogel with ultralow conductive filler content for stretchable electromagnetic interference shielding. *ACS Nano* **2024**, *18*, 2906–2916. DOI:10.1021/acsnano.3c07233
22. Zhang Y, Xu MK, Wang Z, Zhao T, Liu LX, Zhang HB, et al. Strong and conductive reduced graphene oxide-MXene porous films for efficient electromagnetic interference shielding. *Nano Res.* **2022**, *15*, 4916–4924. DOI:10.1007/s12274-022-4311-9
23. Liu Y, Wang Y, Wu N, Han M, Liu W, Liu J, et al. Diverse structural design strategies of MXene-based macrostructure for high-performance electromagnetic interference shielding. *Nano-Micro Lett.* **2023**, *15*, 240. DOI:10.1007/s40820-023-01203-5
24. Zecchi S, Cristoforo G, Bartoli M, Tagliaferro A, Torsello D, Rosso C, et al. A comprehensive review of electromagnetic interference shielding composite materials. *Micromachines* **2024**, *15*, 187. DOI:10.3390/mi15020187
25. Cao Y, Zeng Z, Huang D, Chen Y, Zhang L, Sheng X. Multifunctional phase change composites based on biomass/MXene-derived hybrid scaffolds for excellent electromagnetic interference shielding and superior solar/electro-thermal energy storage. *Nano Res.* **2022**, *15*, 8524–8535. DOI:10.1007/s12274-022-4626-6
26. Tan S, Guo S, Wu Y, Zhang T, Tang J, Ji G. Achieving broadband microwave shielding, thermal management, and smart window in energy-efficient buildings. *Adv. Funct. Mater.* **2025**, *35*, 2415921. DOI:10.1002/adfm.202415921
27. Wang Y, Li J, Li W, Ma L, Lin J, Ye S, et al. Flexible polypyrrole-coated polyamide based mats for broadband microwave absorption and electromagnetic interference shielding with low reflection. *ACS Appl. Polym. Mater.* **2023**, *5*, 2995–3004. DOI:10.1021/acsapm.3c00175

28. Shi S, Jiang Y, Ren H, Deng S, Sun J, Cheng F, et al. 3D-printed carbon-based conformal electromagnetic interference shielding module for integrated electronics. *Nano-Micro Lett.* **2024**, *16*, 85. DOI:10.1007/s40820-023-01317-w
29. Zheng J, Mao S, Zhang S, Liu J, Song Y, Zhang S, et al. Mineral-based electromagnetic wave absorbers and shields: Latest progress and perspectives. *J. Alloys Compd.* **2025**, *1022*, 179884. DOI:10.1016/j.jallcom.2025.179884
30. Ren S, Yu H, Wang L, Huang Z, Lin T, Huang Y, et al. State of the art and prospects in metal-organic framework-derived microwave absorption materials. *Nano-Micro Lett*. **2022**, *14*, 68. DOI:10.1007/s40820-022-00808-6
31. Gao YN, Wang Y, Yue TN, Wang M. Achieving absorption-type electromagnetic shielding performance in silver microtubes/barium ferrites/poly(lactic acid) composites via enhancing impedance matching and electric-magnetic synergism. *Compos. Part B* **2023**, *249*, 110402. DOI:10.1016/j.compositesb.2022.110402
32. Wei H, Zhang Z, Hussain G, Zhou L, Li Q, (Ken) Ostrikov K. Techniques to enhance magnetic permeability in microwave absorbing materials. *Appl. Mater. Today* **2020**, *19*, 100596. DOI:10.1016/j.apmt.2020.100596
33. Xu X, Li D, Li L, Yang Z, Lei Z, Xu Y. Architectural design and microstructural engineering of metal–organic framework-derived nanomaterials for electromagnetic wave absorption. *Small Struct*. **2023**, *4*, 2200219. DOI:10.1002/sstr.202200219
34. Deng W, Li T, Li H, Abdul J, Liu L, Dang A, et al. MOF derivatives with gradient structure anchored on carbon foam for high-performance electromagnetic wave absorption. *Small* **2024**, *20*, 2309806. DOI:10.1002/smll.202309806
35. Feng A, Yu L, Lan D, Lv C, Zhang S, Gao Z, et al. Component modulation strategy to construct multi-heterogeneous interfaces to promote interfacial polarization for efficient electromagnetic wave absorption. *J. Mater. Sci. Technol*. **2025**, *228*, 225–33. DOI:10.1016/j.jmst.2025.02.001
36. Tao J, Xu L, Pei C, Gu Y, He Y, Zhang X, et al. Catfish effect induced by anion sequential doping for microwave absorption. *Adv. Funct. Mater.* **2023**, *33*, 2211996. DOI:10.1002/adfm.202211996
37. Tang Y, Yin P, Zhang L, Wang J, Feng X, Wang K, et al. Novel carbon encapsulated zinc ferrite/MWCNTs composite: Preparation and low-frequency microwave absorption investigation. *Ceram. Int*. **2020**, 46, 28250–28261. DOI:10.1016/j.ceramint.2020.07.326
38. Bu A, Zhang Y, Xiang Y, Chen W, Cheng H, Wang L. Enhanced antioxidation and microwave absorbing properties of SiC/SiO_2 coating on carbon fiber. *J Mater. Sci. Mater. Electron.* **2020**, *31*, 17067–17074. DOI:10.1007/s10854-020-04264-z
39. Wang J, Wang B, Feng A, Jia Z, Wu G. Design of morphology-controlled and excellent electromagnetic wave absorption performance of sheet-shaped $ZnCo_2O_4$ with a special arrangement. *J. Alloys Compd*. **2020**, *834*, 155092. DOI:10.1016/j.jallcom.2020.155092
40. Meng X, Zhang T, Zhang J, Qu G, Wu L, Liu H, et al. Deformable BCN/Fe_3O_4/PCL composites through electromagnetic wave remote control. *Nanotechnology* **2020**, *31*, 255710. DOI:10.1088/1361-6528/ab758c
41. Yin P, Zhang L, Sun P, Wang J, Feng X, Zhang Y, et al. Apium-derived biochar loaded with $MnFe_2O_4$@C for excellent low frequency electromagnetic wave absorption. *Ceram. Int.* **2020**, *46*, 13641–13650. DOI:10.1016/j.ceramint.2020.02.150
42. Huo J, Wang L, Yu H. Polymeric nanocomposites for electromagnetic wave absorption. *J. Mater. Sci.* **2009**, *44*, 3917–3927. DOI:10.1007/s10853-009-3561-1
43. Wu T, Liu Y, Zeng X, Cui T, Zhao Y, Li Y, et al. Facile hydrothermal synthesis of Fe_3O_4/C core–shell nanorings for efficient low-frequency microwave absorption. *ACS Appl. Mater. Interfaces* **2016**, *8*, 7370–7380. DOI:10.1021/acsami.6b00264
44. Zhao S, Wang C, Zhong B. Optimization of electromagnetic wave absorbing properties for Ni-Co-P/GNs by controlling the content ratio of Ni to Co. *J. Magn. Magn. Mater.* **2020**, *495*, 165753. DOI:10.1016/j.jmmm.2019.165753
45. Zhao B, Deng J, Zhang R, Liang L, Fan B, Bai Z, et al. Recent advances on the electromagnetic wave absorption properties of Ni based materials. *Eng. Sci.* **2018**, *3*, 5–40. DOI:10.30919/es8d735
46. Liang W, Wu J, Zhang S, Zhao PY, Cong Y, Guo Y, et al. Porous $Ti_3C_2T_x$ MXene nanosheets sandwiched between polyimide fiber mats for electromagnetic interference shielding. *Nano Res.* **2024**, *17*, 2070–2078. DOI:10.1007/s12274-023-6405-4
47. Lin J, Huang J, Guo Z, Xu BB, Cao Y, Ren J, et al. Hydrophobic multilayered PEG@PAN/MXene/PVDF@SiO_2 composite film with excellent thermal management and electromagnetic interference shielding for electronic devices. *Small* **2024**, *20*, 2402938. DOI:10.1002/smll.202402938
48. Jia F, Lu Z, Huang T, Xu M, Xu X, Guo Z, et al. Twin-coated skeleton PEDOT: PSS/MXene/para-aramid nanofibers hybrid aerogel with efficient EMI shielding performance and tunable power coefficient. *Adv. Compos. Hybrid Mater.* **2025**, *8*, 200. DOI:10.1007/s42114-025-01290-5
49. Xie Y, Liu S, Huang K, Chen B, Shi P, Chen Z, et al. Ultra-broadband strong electromagnetic interference shielding with ferromagnetic graphene quartz fabric. *Adv. Mater.* **2022**, *34*, 2202982. DOI:10.1002/adma.202202982

50. Hong J, Kwon J, Im D, Ko J, Nam CY, Yang HG, et al. Best practices for correlating electrical conductivity with broadband EMI shielding in binary filler-based conducting polymer composites. *Chem. Eng. J.* **2023**, *455*, 140528. DOI:10.1016/j.cej.2022.140528
51. Guo Y, Chen X, Wei C, Luo Y, Chen J, Zhu Y. Flexible conductive polymer composite film with sandwich-like structure for ultra-efficient and high-stability electromagnetic interference shielding. *Compos. Sci. Technol.* **2024**, *255*, 110717. DOI:10.1016/j.compscitech.2024.110717
52. Deng F, Wei J, Xu Y, Lin Z, Lu X, Wan YJ, et al. Regulating the electrical and mechanical properties of TaS_2 films via van der waals and electrostatic interaction for high performance electromagnetic interference shielding. *Nano-Micro Lett.* **2023**, *15*, 106. DOI:10.1007/s40820-023-01061-1
53. Wang Q, Niu B, Han Y, Zheng Q, Li L, Cao M. Nature-inspired 3D hierarchical structured "vine" for efficient microwave attenuation and electromagnetic energy conversion device. *Chem. Eng. J.* **2023**, *452*, 139042. DOI:10.1016/j.cej.2022.139042
54. Kang BH, Lee DK, Kim D, Hur ON, Lee CS, Bae J, et al. High-yield exfoliation of $NbSe_2$ through optimized lithium-ion intercalation and its application in electromagnetic-interference shielding. *Appl. Surf. Sci.* **2023**, *637*, 157954. DOI:10.1016/j.apsusc.2023.157954
55. Zhou Y, Zhang X, Ma J, Zhao J. Preparation and properties of electromagnetic shielding leather based on magnetic MgFeCr-LDHs. *J. Environ. Chem. Eng.* **2024**, *12*, 113394. DOI:10.1016/j.jece.2024.113394
56. Li Y, Liu J, Zhang M, Ren Y, Shen B, Chen J, et al. Carbon fabric composites with NiCo compounds: Structure evolution and EMI shielding performance. *Appl. Surf. Sci.* **2023**, *627*, 157275. DOI:10.1016/j.apsusc.2023.157275
57. Liao F, Xu Z, Fan Z, Meng Q, Lv B, Zhang GL, et al. Confined assembly of ultrathin dual-functionalized Z-MXene nanosheet intercalated GO nanofilms with controlled structure for size-selective permeation. *J. Mater. Chem. A* **2021**, *9*, 12236–12243. DOI:10.1039/D1TA01514A
58. Xu Z, Chen Y, Meng Q, Yang A, Zhang H, Zhang GL. N/P co-doped MXene hollow microcapsules by surfactants assisted hydrothermal-freeze drying for adjustable permeability. *Nanotechnology* **2024**, *35*, 125604. DOI:10.1088/1361-6528/ad1648
59. Xu Z, Zhang Y, Liu M, Meng Q, Shen C, Zhang GL, et al. Two-dimensional titanium carbide MXene produced by ternary cations intercalation via structural control with angstrom-level precision. *iScience* **2022**, *25*, 105562. DOI:10.1016/j.isci.2022.105562
60. Zhang GL, Wang T, Xu Z, Liu M, Shen C, Meng Q. Synthesis of amino-functionalized $Ti_3C_2T_x$ MXene by alkalization-grafting modification for efficient lead adsorption. *Chem. Commun.* **2020**, *56*, 11283–11286. DOI:10.1039/D0CC04265J
61. Duan H, Wang C, Yi Y, Mu X, Ding H, Bi Z, et al. Scalable, mechanically-robust, fire-resistance MXene/PEDOT:PSS/PBO film for efficient electromagnetic interference shielding and joule heating performance. *Chem. Eng. J.* **2024**, *483*, 149302. DOI:10.1016/j.cej.2024.149302
62. Yang Y, Wu N, Li B, Liu W, Pan F, Zeng Z, et al. Biomimetic porous MXene sediment-based hydrogel for high-performance and multifunctional electromagnetic interference shielding. *ACS Nano* **2022**, *16*, 15042–15052. DOI:10.1021/acsnano.2c06164
63. Malik R, Parida RK, Parida BN, Nayak NC. EMI shielding behavior of 2D-layered $Ti_3C_2T_x$ (MXene) incorporated EMA/EOC ternary blend nanocomposites in S-band. *J. Mater. Sci. Mater. Electron.* **2022**, *33*, 22599–22613. DOI:10.1007/s10854-022-09038-3
64. Chen Q, Fan B, Zhang Q, Wang S, Cui W, Jia Y, et al. Design of 3D lightweight $Ti_3C_2T_x$ MXene porous film with graded holes for efficient electromagnetic interference shielding performance. *Ceram. Int.* **2022**, *48*, 14578–14586. DOI:10.1016/j.ceramint.2022.01.351
65. Zhang J, Zhang S, Song Y, Weng Y, Liang Y, Wu Z, et al. Surface structure engineering and electromagnetic character regulation synergestically boosts electromagnetic shielding performances of carbon nanotube sponge. *Carbon* **2025**, *233*, 119879. DOI:10.1016/j.carbon.2024.119879
66. Xiang Z, Wang X, Zhang X, Shi Y, Cai L, Zhu X, et al. Self-assembly of nano/microstructured 2D Ti_3CNT_x MXene-based composites for electromagnetic pollution elimination and joule energy conversion application. *Carbon* **2022**, *189*, 305–318. DOI:10.1016/j.carbon.2021.12.075
67. Wen Y, Bian H, Ran Y, Xie Y, You M, Wen H, et al. $Ti_3C_2T_x$ MXene/FeCo/Ni flakes composites with convenient preparation process for broadband electromagnetic shielding. *Mater. Today Commun.* **2025**, *43*, 111689. DOI:10.1016/j.mtcomm.2025.111689
68. Hu Y, Hou C, Shi Y, Wu J, Yang D, Huang Z, et al. Freestanding $Fe_3O_4/Ti_3C_2T_x$ MXene/polyurethane composite film with efficient electromagnetic shielding and ultra-stretchable performance. *Nanotechnology* **2022**, *33*, 165603. DOI:10.1088/1361-6528/ac4878

69. Xu X, Zhang R, Li X, Zhang G, Yang Y, Xia L, et al. Tailored hard/soft magnetic heterostructure anchored on 2D carbon nanosheet for efficient microwave absorption and anti-corrosion property. *Nano Res.* **2025**, *18*, 94907363. DOI:10.26599/NR.2025.94907363
70. Lou L, Al-Duhni GSG, Cruz OB, Volakis JL, Pulugurtha M, Agarwal A. Iron oxide quantum dots and graphene nanoplatelets integrated in a dual-polymer conductive fiber for electromagnetic interference-shielding thin films. *ACS Appl. Nano Mater.* **2025**, *8*, 3617–3630. DOI:10.1021/acsanm.4c07086
71. Hua T, Guo H, Qin J, Wu Q, Li L, Qian B. 3D printing lamellar $Ti_3C_2T_x$ MXene/graphene hybrid aerogels for enhanced electromagnetic interference shielding performance. *RSC Adv.* **2022**, *12*, 24980–24987. DOI:10.1039/D2RA02951K
72. He P, Liu Z, Yu J, Yan Y, Kong H, Zhao B, et al. Synergistically engineered PVDF/CNT/GnP hierarchical nanocomposites via scalable solution spinning for ultradurable, superhydrophobic EMI shielding wearables. *J. Mater. Chem. C* **2025**, *13*, 12242–12253. DOI:10.1039/D5TC01041A
73. Haspulat Taymaz B, Eskizeybek V. Lightweight and sustainable recycled cellulose based hybrid aerogels with enhanced electromagnetic interference shielding. *Cellulose* **2025**, *32*, 3335–3354. DOI:10.1007/s10570-025-06471-5
74. Mehmood Z, Shah SAA, Omer S, Idrees R, Saeed S. Scalable synthesis of high-quality, reduced graphene oxide with a large C/O ratio and its dispersion in a chemically modified polyimide matrix for electromagnetic interference shielding applications. *RSC Adv.* **2024**, *14*, 7641–7654. DOI:10.1039/D4RA00329B
75. Bai W, Zhai J, Zhou S, Cui C, Wang W, Cheng C, et al. Graphene oxide nanosheets and Ni nanoparticles coated on glass fabrics modified with bovine serum albumin for electromagnetic shielding. *ACS Appl. Nano Mater.* **2022**, *5*, 8491–8501. DOI:10.1021/acsanm.2c01760
76. Yao L, Wang Y, Zhao J, Zhu Y, Cao M. Multifunctional nanocrystalline-assembled porous hierarchical material and device for integrating microwave absorption, electromagnetic interference shielding, and energy storage. *Small* **2023**, *19*, 2208101. DOI:10.1002/smll.202208101
77. Yan R, Huang Z, Chen Y, Zhang L, Sheng X. Phase change composite based on lignin carbon aerogel/nickel foam dual-network for multisource energy harvesting and superb EMI shielding. *Int. J. Biol. Macromol.* **2024**, *277*, 134233. DOI:10.1016/j.ijbiomac.2024.134233
78. Liu T, Wang Y, Wang Y, Cao M. "Heterodimensional structure" integrated defect and interface engineering for efficiently EMI shielding and electrochemical response. *Adv. Funct. Mater.* **2025**, *35*, 2404280. DOI:10.1002/adfm.202404280
79. Kim WJ, Nam KW, Park SH. Enhanced electromagnetic shielding via sequential exfoliation of $NbSe_2$ thin film: Structural and electrical optimization. *Electron. Mater. Lett.* **2025**, *21*, 707–714. DOI:10.1007/s13391-025-00585-5
80. Luxa J, Oliveira FM, Jellet CW, Gusmão R, Sofer Z. Freestanding foils of $NbSe_2$ and carbon nanotubes for efficient electromagnetic shielding. *ACS Appl. Nano Mater.* **2023**, *6*, 3333–3343. DOI:10.1021/acsanm.2c05119
81. Sharma S, Pratap Singh B, Hur SH, Choi WM, Chung JS. Facile fabrication of stacked rGO/MoS_2 reinforced polyurethane composite foam for effective electromagnetic interference shielding. *Compos. Part A* **2023**, *166*, 107366. DOI:10.1016/j.compositesa.2022.107366
82. Zhu Y, Liu T, Li L, Cao M. Multifunctional WSe_2/Co_3C composite for efficient electromagnetic absorption, EMI shielding, and energy conversion. *Nano Res.* **2024**, *17*, 1655–1665. DOI:10.1007/s12274-023-6272-z
83. Ghosh S, Aboulsaad MM, Slimani S, Cedervall J, Aslibeiki B, Edvinsson T, et al. Triphasic inter-dimensional WS_2/magnetic lithium iron oxide nanocomposite for electromagnetic interference shielding. *Adv. Mater. Interfaces* **2025**, *12*, e00687. DOI:10.1002/admi.202500687
84. Daniel S, Joseph S, Alapat PS, Kalarikkal N, Thomas S. Silver-sandwiched natural rubber/st-LDH/MWCNT hybrid bio-nano-composite system as a high-performing multimedia laminated electromagnetic interference shield through a tripling mechanism. *ACS Sustain. Chem. Eng.* **2022**, *10*, 14897–14913. DOI:10.1021/acssuschemeng.2c04820
85. Qin Q, Hu Y, Sun N, Lei T, Yang Y, Cui Z, et al. Fabrication of PVA-based electromagnetic interference shielding composite film by improving the dispersibility of carbon nanomaterial via m-LDH modification. *Chem. Eng. J.* **2024**, *490*, 151611. DOI:10.1016/j.cej.2024.151611
86. Shi Y, Nie C, Jiang S, Wang H, Feng Y, Gao J, et al. Tunable construction of fire safe and mechanically strong hierarchical composites towards electromagnetic interference shielding. *J. Colloid Interface Sci.* **2023**, *652*, 1554–1567. DOI:10.1016/j.jcis.2023.08.191
87. Lyu B, Chen K, Zhu J, Gao D. Multifunctional wearable electronic based on fabric modified by PPy/NiCoAl-LDH for energy storage, electromagnetic interference shielding, and photothermal conversion. *Small* **2024**, *20*, 2402510. DOI:10.1002/smll.202402510
88. Duan Y, Yang W, Zhang Y, Gu Y, Xu P, Niu D, et al. Advanced hollow ball-cactus-like soft-magnetic LDH@MXeneHT nanohybrid materials towards highly efficient electromagnetic protection. *Compos. Part B* **2025**, *306*, 112807. DOI:10.1016/j.compositesb.2025.112807

89. Wang Z, Wang R, Gao G, Wang Z, Peng H, Cao H, et al. Comprehensive performance evaluation of HGM hybrid modified resins: Excellent high resistivity terahertz shielding and impact energy absorption properties. *Polym. Compos*. **2024**, *45*, 16832–16849. DOI:10.1002/pc.28935
90. Ghamarpoor R, Jamshidi M, Kandelousi DM. Electromagnetic interference (EMI) shielding, electrical, thermal, and mechanical properties of silanized hexagonal boron nitride (h-BN) heterostructures and decorated by ag nanoparticles: Towards smart coatings. *J. Alloys Compd*. **2025**, *1020*, 179561. DOI:10.1016/j.jallcom.2025.179561
91. Chen X, Guo Y, Zhang Y, Wang Y, Hou M, Chen J, et al. Electric insulation, high thermal conductivity, and ultra-high EMI shielding composite films with a janus structure. *Compos. Sci. Technol.* **2026**, *273*, 111423. DOI:10.1016/j.compscitech.2025.111423
92. Fan G, Xiong T, Mouldi A, Bouallegue B, Tran N, Mahmoud MZ. Enhanced electromagnetic interference shielding effectiveness of h-BN decorated micro cube-like $CaTiO_3$/Cu nanocomposite. *Ceram. Int*. **2022**, *48*, 8529–8539. DOI:10.1016/j.ceramint.2021.12.063
93. Feng L, Wei P, Song Q, Zhang J, Fu Q, Jia X, et al. Superelastic, highly conductive, superhydrophobic, and powerful electromagnetic shielding hybrid aerogels built from orthogonal graphene and boron nitride nanoribbons. *ACS Nano* **2022**, *16*, 17049–17061. DOI:10.1021/acsnano.2c07187
94. Guo Y, Wang D, Wang J, Tian Y, Liu H, Liu C, et al. Hierarchical HCF@NC/Co derived from hollow loofah fiber anchored with metal–organic frameworks for highly efficient microwave absorption. *ACS Appl. Mater. Interfaces* **2022**, *14*, 2038–2050. DOI:10.1021/acsami.1c21396
95. Jiao Y, Wu F, Xie A, Wu L, Zhao W, Zhu X, et al. Electrically conductive conjugate microporous polymers (CMPs) via confined polymerization of pyrrole for electromagnetic wave absorption. *Chem. Eng. J*. **2020**, *398*, 125591. DOI:10.1016/j.cej.2020.125591
96. Wang K, Zhou Q, Liu H, Xie A, Naqvi QA, Wang W, et al. CNT-coupled 2D-MOF composite materials enable tunable bandwidth electromagnetic wave absorption. *Mater. Today Nano* **2025**, *29*, 100605. DOI:10.1016/j.mtnano.2025.100605
97. Yan J, Wang Y, Liu W, Liu P, Chen W. Two-dimensional metal organic framework derived nitrogen-doped graphene-like carbon nanomesh toward efficient electromagnetic wave absorption. *J. Colloid Interface Sci.* **2023**, *643*, 318–327. DOI:10.1016/j.jcis.2023.04.040
98. Cui Z, Gao C, Fan Z, Wang J, Cheng Z, Xie Z, et al. Lightweight MXene/cellulose nanofiber composite film for electromagnetic interference shielding. *J. Electron. Mater.* **2021**, *50*, 2101–2110. DOI:10.1007/s11664-020-08718-2
99. He J, Zhang H, Chen Y, Zou H, Liang M. Bi-continuous conductive network induced by *in-situ* phase separation in epoxy composites with enhanced electromagnetic interference shielding performance. *React. Funct. Polym.* **2021**, *164*, 104918. DOI:10.1016/j.reactfunctpolym.2021.104918
100. Hong X, Peng T, Zhu C, Wan J, Li Y. Electromagnetic shielding, resistance temperature-sensitive behavior, and decoupling of interfacial electricity for reduced graphene oxide paper. *J. Alloys Compd.* **2021**, *882*, 160756. DOI:10.1016/j.jallcom.2021.160756
101. Huang J, Wang T, Su Y, Ding Y, Tu C, Li W. Hydrophobic MXene/hydroxyethyl cellulose/silicone resin composites with electromagnetic interference shielding. *Adv. Mater. Interfaces* **2021**, *8*, 2100186. DOI:10.1002/admi.202100186
102. Jiang Y, Liang M, Wang W, Lai X, Xie K, Liao L, et al. Porous nano-Ni/graphene/loofah composites for electromagnetic interference shielding. *Int. J. Precis. Eng. Manuf.-Green Technol.* **2022**, *9*, 1121–1132. DOI:10.1007/s40684-021-00375-y
103. Wang Y, Qi Q, Yin G, Wang W, Yu D. Flexible, ultralight, and mechanically robust waterborne polyurethane/$Ti_3C_2T_x$ MXene/nickel ferrite hybrid aerogels for high-performance electromagnetic interference shielding. *ACS Appl. Mater. Interfaces* **2021**, *13*, 21831–21843. DOI:10.1021/acsami.1c04962
104. Yang H, Wang L, Wang H, Zhang Y, Su Z, Su Z, et al. Transparent and high-absolute-effectiveness electromagnetic interference shielding film based on single-crystal graphene. *Adv. Mater. Technol.* **2022**, *7*, 2101465. DOI:10.1002/admt.202101465
105. Jiang Y, Wang W, Liang M, Lai X, Xie K, Liao L, et al. 3D hierarchical porous composites based on natural loofahs/cobalt nanoparticles/graphene oxide with efficient electromagnetic interference shielding performance. *J. Alloys Compd.* **2021**, *889*, 161716. DOI:10.1016/j.jallcom.2021.161716
106. Yao Y, Jin S, Wang M, Gao F, Xu B, Lv X, et al. MXene hybrid polyvinyl alcohol flexible composite films for electromagnetic interference shielding. *Appl. Surf. Sci.* **2022**, *578*, 152007. DOI:10.1016/j.apsusc.2021.152007
107. Zhou J, Yuan B, Tao H, Chen G, Zhan Y, Wang Y, et al. The design of lightweight and porous graphene-based composite paper and the study on its electromagnetic interference shielding and fire resistance. *Mater. Lett.* **2021**, *304*, 130625. DOI:10.1016/j.matlet.2021.130625
108. Bai Y, Ju J, Pan Y, Zhang B, Yan Y, Fei G. Shape memory-driven intelligent composite film for infrared stealth and adjustable EMI shielding. *Small* **2026**, *22*, e10825. DOI:10.1002/smll.202510825

109. Tao D, Wen X, Ma S, Chen C, Guo J, Wang W, et al. High electrical conductivity induced by surface confinement effect in heterostructured multifunctional nanofiber composite films for low-reflection electromagnetic interference shielding. *Adv. Sci.* **2025**, *12*, e10386. DOI:10.1002/advs.202510386
110. Ma L, Hamidinejad M, Zhao B, Liang C, Park CB. Layered foam/film polymer nanocomposites with highly efficient EMI shielding properties and ultralow reflection. *Nano-Micro Lett.* **2022**, *14*, 19. DOI:10.1007/s40820-021-00759-4
111. Lu Z, Jia F, Zhuo L, Ning D, Gao K, Xie F. Micro-porous MXene/Aramid nanofibers hybrid aerogel with reversible compression and efficient EMI shielding performance. *Compos. Part B Eng.* **2021**, *217*, 108853. DOI:10.1016/j.compositesb.2021.108853
112. Gao Q, Qin J, Guo B, Fan X, Wang F, Zhang Y, et al. High-performance electromagnetic interference shielding epoxy/Ag nanowire/thermal annealed graphene aerogel composite with bicontinuous three-dimensional conductive skeleton. *Compos. Part A* **2021**, *151*, 106648. DOI:10.1016/j.compositesa.2021.106648
113. Jia H, Yi ZL, Huang XH, Su FY, Kong QQ, Yang X, et al. A one-step graphene induction strategy enables *in-situ* controllable growth of silver nanowires for electromagnetic interference shielding. *Carbon* **2021**, *183*, 809–819. DOI:10.1016/j.carbon.2021.07.067
114. Liu H, Xu Y, Cao JP, Han D, Yang Q, Li R, et al. Skin structured silver/three-dimensional graphene/polydimethylsiloxane composites with exceptional electromagnetic interference shielding effectiveness. *Compos. Part A* **2021**, *148*, 106476. DOI:10.1016/j.compositesa.2021.106476
115. Sun L, Liu R, Ma Y, Wang W, Yuan Y, Zhang H, et al. Flexible and hydrophobic CoFe-LDH @Co MOF @biomass-derived carbon fabrics for effective near-infrared photothermal conversion and electromagnetic attenuation. *J. Alloys Compd.* **2024**, *1002*, 175518. DOI:10.1016/j.jallcom.2024.175518
116. Song C, Meng X, Chen H, Liu Z, Zhan Q, Sun Y, et al. Flexible, graphene-based films with three-dimensional conductive network via simple drop-casting toward electromagnetic interference shielding. *Compos. Commun.* **2021**, *24*, 100632. DOI:10.1016/j.coco.2021.100632
117. Shi Y, Wu S, Chen J, Tang L, Gao J, Zou H, et al. Hierarchically building flame retardant and flexible electromagnetic interference shielding composites with tunable mechanism. *J. Mater. Sci. Technol.* **2025**, *239*, 39–54. DOI:10.1016/j.jmst.2025.03.053
118. Shi Y, You X, Niu H, Liao C, Tang L, Gao J, et al. Highly effective core-shell CNF/HGM@CS/MXene electromagnetic interference composite films with superior flame retardancy. *Chem. Eng. J.* **2026**, *533*, 174979. DOI:10.1016/j.cej.2026.174979
119. Zhao P, Gao D, Zhou Y, Lyu B, Ma J. Multifunctional integrated flexible triboelectric nanogenerator based on collagen fibers for smart wearable devices. *Chem. Eng. J.* **2025**, *522*, 167693. DOI:10.1016/j.cej.2025.167693
120. Wang S, Sun Z, Wang Y, Liang T, Wang B, Fan C, et al. Design of CuS composite carbon-based Ni Al-LDH multifunctional phase change composite with electromagnetic shielding performance and heat storage capacity. *Chem. Eng. J.* **2024**, *491*, 151960. DOI:10.1016/j.cej.2024.151960
121. Zhao B, Wu H, Tian Q, Li Y, Qiu F, Zhang T. Laminated MXene foam/cellulose@LDH composite membrane with efficient EMI shielding property for asymmetric personal thermal management. *ACS Appl. Mater. Interfaces* **2023**, *15*, 8751–8760. DOI:10.1021/acsami.2c21694
122. Zhao P, Gao D, Lyu B, Ma J, Kim K-H. Fabrication of effective electromagnetic shielding leather with a chromium-free multi-network structure. *J. Clean. Prod.* **2022**, *374*, 133856. DOI:10.1016/j.jclepro.2022.133856
123. Li W, Yin Z, Qi L, Yu B, Xing W. Scalable production of bioinspired MXene/black phosphorene nanocoatings for hydrophobic and fire-safe textiles with tunable electromagnetic interference and exceeding thermal management. *Chem. Eng. J.* **2023**, *460*, 141870. DOI:10.1016/j.cej.2023.141870
124. Wen C, Zhao B, Liu Y, Xu C, Wu Y, Cheng Y, et al. Flexible MXene-based composite films for multi-spectra defense in radar, infrared and visible light bands. *Adv. Funct. Mater.* **2023**, *33*, 2214223. DOI:10.1002/adfm.202214223
125. Bai W, Zhai J, Zhou S, Cui C, Wang W, Jiang S, et al. Flexible MOF on $Co_XFe_{1-X}OOH$@biomass derived alloy@carbon films for efficient electromagnetic interference shielding and energy conversion. *Carbon* **2022**, *199*, 96–109. DOI:10.1016/j.carbon.2022.07.059
126. Gao T, Zhao H, Lv Y, Zhang J, Kong J, Zhuang Q, et al. Cobalt nanoparticles/nitrogen-doped reduced graphene oxide composite films for efficient electromagnetic shielding. *ACS Appl. Nano Mater.* **2026**, *9*, 332–342. DOI:10.1021/acsanm.5c04531
127. Gui J, Wang L, Li Y, Yang L, Yu D, Wang W. BN@MXene porous thermal conductive composites based on thiol-ene click chemistry and 3D printing for absorption-oriented electromagnetic shielding. *Chem. Eng. J.* **2025**, *522*, 167547. DOI:10.1016/j.cej.2025.167547

128. Kim S, Lee W, Lee J, Kim J. Multifunctional PCM composites for thermal management based on TiO_2-grown carbonized cotton and acetamide grafted Bisphenol-A. *Carbon* **2026**, *247*, 121038. DOI:10.1016/j.carbon.2025.121038
129. Seol M, Hwang U, Kim J, Eom D, Park IK, Kim H, et al. Solution printable multifunctional polymer-based composites for smart electromagnetic interference shielding with tunable frequency and on–off selectivities. *Adv. Compos. Hybrid Mater.* **2023**, *6*, 46. DOI:10.1007/s42114-022-00609-w
130. Su Z, Yang H, Wang G, Zhang Y, Zhang J, Lin J, et al. Transparent and high-performance electromagnetic interference shielding composite film based on single-crystal graphene/hexagonal boron nitride heterostructure. *J. Colloid Interface Sci.* **2023**, *640*, 610–618. DOI:10.1016/j.jcis.2023.02.115
131. Yun J, Lee J, Kim J, Lee J, Choi W. Hexagonal boron nitride nanosheets/graphene nanoplatelets/cellulose nanofibers-based multifunctional thermal interface materials enabling electromagnetic interference shielding and electrical insulation. *Carbon* **2024**, *228*, 119397. DOI:10.1016/j.carbon.2024.119397
132. Lee HR, Choi TM, Pyo SG. Multifunctional ceramic-based nanocomposites for advanced electromagnetic interference shielding in stealth applications. *J. Alloys Compd*. **2025**, *1047*, 185136. DOI:10.1016/j.jallcom.2025.185136
133. Wang H, Wang B, Su B, Cao Y, Hou L. Carbon nanotubes and montmorillonite reinforced carbon foam composites containing hollow microspheres. *Carbon Lett.* **2024**, *34*, 1755–1764. DOI:10.1007/s42823-024-00727-z
134. Dang W, Liu Z, Wang L, Chen Y, Qi M, Zhang Q. A flexible, robust and multifunctional montmorillonite/aramid nanofibers@MXene electromagnetic shielding nanocomposite with an alternating structure for enhanced joule heating and fire-resistant protective performance. *Nanoscale* **2022**, *14*, 11305–11315. DOI:10.1039/D2NR01926D
135. Jiang X, Yan DX, Bao Y, Pang H, Ji X, Li ZM. Facile, green and affordable strategy for structuring natural graphite/polymer composite with efficient electromagnetic interference shielding. *RSC Adv.* **2015**, *5*, 22587–22592. DOI:10.1039/C4RA11332B
136. Cheng R, Wu Y, Wang B, Zeng J, Li J, Xu J, et al. Fireproof ultrastrong all-natural cellulose nanofiber/montmorillonite-supported MXene nanocomposites with electromagnetic interference shielding and thermal management multifunctional applications. *J. Mater. Chem. A* **2023**, *11*, 18323–18335. DOI:10.1039/D3TA03798C
137. Li J, Xu P, Zhang Y, Tian N, Su Z, Huang Q. *In-situ* synthesis of a novel MG@SiC-NWs composite with excellent electromagnetic wave absorption properties by carbothermal reduction using natural microcrystalline graphite. *Ceram. Int.* **2025**, *51*, 39069–39080. DOI:10.1016/j.ceramint.2025.06.146
138. Kumari P, Tripathi P, Parkash O, Kumar D. Electromagnetic interference shielding effectiveness of $MgO{-}Al_2O_3{-}SiO_2$ glass–ceramic system. *Bull. Mater. Sci.* **2017**, *40*, 1497–1501. DOI:10.1007/s12034-017-1505-y
139. Li YM, Deng C, Zhao ZY, Han LX, Lu P, Wang YZ. Carbon fiber-based polymer composite via ceramization toward excellent electromagnetic interference shielding performance and high temperature resistance. *Compos. Part A* **2020**, *131*, 105769. DOI:10.1016/j.compositesa.2020.105769
140. Peng HK, Wang XX, Li TT, Huang SY, Lin Q, Shiu BC, et al. Effects of hydrotalcite on rigid polyurethane foam composites containing a fire retarding agent: Compressive stress, combustion resistance, sound absorption, and electromagnetic shielding effectiveness. *RSC Adv.* **2018**, *8*, 33542–33550. DOI:10.1039/C8RA06361C
141. Darvishzadeh A, Nasouri K. Structural engineering of nickel-coated carbon fibers with high electrical conductivity for flexible EMI shielding. *J. Mater. Sci: Mater. Electron.* **2022**, *33*, 5648–5660. DOI:10.1007/s10854-022-07751-7
142. Lu J, Zhang Y, Tao Y, Wang B, Cheng W, Jie G, et al. Self-healable castor oil-based waterborne polyurethane/MXene film with outstanding electromagnetic interference shielding effectiveness and excellent shape memory performance. *J. Colloid Interface Sci.* **2021**, *588*, 164–174. DOI:10.1016/j.jcis.2020.12.076
143. Zhao J, Lai H, Li M. Anchoring 1T-MoS_2 petals on N-doped reduced graphene oxide for exceptional electromagnetic wave absorption. *Int. J. Miner. Metall. Mater.* **2025**, *32*, 619–630. DOI:10.1007/s12613-024-2998-1
144. Xiang Z, Shi Y, Zhu X, Cai L, Lu W. Flexible and waterproof 2D/1D/0D construction of MXene-based nanocomposites for electromagnetic wave absorption, EMI shielding, and photothermal conversion. *Nano-Micro Lett.* **2021**, *13*, 150. DOI:10.1007/s40820-021-00673-9
145. Zhang S, Jia Z, Zhang Y, Wu G. Electrospun $Fe_{0.64}Ni_{0.36}$/MXene/CNFs nanofibrous membranes with multicomponent heterostructures as flexible electromagnetic wave absorbers. *Nano Res*. **2023**, *16*, 3395–3407. DOI:10.1007/s12274-022-5368-1
146. Fan Z, Wang D, Yuan Y, Wang Y, Cheng Z, Liu Y, et al. A lightweight and conductive MXene/graphene hybrid foam for superior electromagnetic interference shielding. *Chem. Eng. J.* **2020**, *381*, 122696. DOI:10.1016/j.cej.2019.122696
147. Zhang S, Li M, Chen G, Wang H, Shao G, Lan D, et al. Achieving high performance microwave attenuation by anchoring magnetic coni nanoparticles onto few-layer $Ti_3C_2T_x$mxene. *J. Alloys Compd.* **2025**, *1805*, 180015. DOI:10.2139/ssrn.5091053

148. Antonets IV, Golubev YA, Shcheglov VI, Sun S. Electromagnetic shielding effectiveness of lightweight and flexible ultrathin shungite plates. *Curr. Appl. Phys.* **2021**, *29*, 97–106. DOI:10.1016/j.cap.2021.06.008
149. Liu X, Zhou J, Xue Y, Lu X. Structural engineering of hierarchical magnetic/carbon nanocomposites via *in situ* growth for high-efficient electromagnetic wave absorption. *Nano-Micro Lett.* **2024**, *16*, 174. DOI:10.1007/s40820-024-01396-3
150. Shan Z, Cheng S, Wu F, Pan X, Li W, Dong W, et al. Electrically conductive two-dimensional metal-organic frameworks for superior electromagnetic wave absorption. *Chem. Eng. J.* **2022**, *446*, 137409. DOI:10.1016/j.cej.2022.137409
151. Wu M, Liang X, Pan S, Wang H, Man Z. Rational design of MoS_2/CoNi heterogeneous for superior electromagnetic wave absorption performance. *J. Alloys Compd.* **2025**, *1048*, 185253. DOI:10.1016/j.jallcom.2025.185253